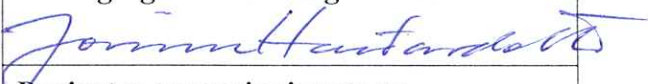Veðurstofa
Íslands

Estimating the flood frequency distribution for ungauged catchments using an index flood procedure. Application to ten catchments in Northern Iceland

Philippe Crochet

Veðurstofa
Íslands

Estimating the flood frequency distribution for ungauged catchments using an index flood procedure. Application to ten catchments in Northern Iceland

Philippe Crochet, Icelandic Met Office

Keypage

Veðurstofa
Íslands

Report no.:	Date:	ISSN:	Public ☒ Restricted ☐
VÍ 2012-005	June 2012	1670-8261	Provision:

Report title / including subtitle	No. of copies: 20
Estimating the flood frequency distribution for ungauged catchments using an index flood procedure. Application to ten catchments in Northern Iceland	Pages: 59
	Managing director: Jórunn Harðardóttir

Author(s):	Project manager:
Philippe Crochet	Philippe Crochet
	Project number: 4812

Project phase:	Case number:

Report contracted for:
Vegagerðin

Prepared in cooperation with:

Summary:

The goal of this study is to develop an objective methodology for estimating design floods, *i.e.* the flood peak discharge with return period T, at poorly gauged and ungauged river catchments in Iceland. This is done by scaling a regional flood frequency distribution by the so-called index flood of the catchment. The regional flood frequency distribution is a dimensionless probability distribution function (PDF) estimated by pooling together the individual flood frequency distributions of a group of homogeneous gauged catchments. The index flood is defined as the mean annual maximum flood peak discharge. For gauged catchments, the index flood is estimated from the measured streamflow series. For ungauged catchments, it is estimated by linear regression using physiographic and climatic catchment descriptors. The method is evaluated for ten catchments located in the Tröllaskagi region and in the West-fjords using annual maximum instantaneous and daily streamflow series. The results indicate that the method looks promising for the estimation of the T-year flood peak discharge and the associated confidence interval, along river channels. This methodology should be further developed and tested in other regions.

Keywords:	Managing director's signature:
Iceland, PUB, regional flood frequency analysis, index flood	*[signature]*
	Project manager's signature: *[signature]*
	Reviewed by: Tómas Jóhannesson, Ásdís Helgadóttir

3

Contents

Abstract

The goal of this study is to develop an objective methodology for estimating design floods, *i.e.* the flood peak discharge with return period T, at ungauged river catchments in Iceland. First, a regional flood frequency analysis is presented for estimating the T-year flood peak discharge with fixed duration D, $\mathrm{Q}(T,D)$, for poorly gauged and ungauged catchments. This is done by scaling a regional flood frequency distribution by the so-called index flood of the catchment. The regional flood frequency distribution is a dimensionless probability distribution function (PDF) estimated by pooling together the individual flood frequency distributions of a group of homogeneous gauged catchments. The index flood is defined here as the mean annual maximum flood peak discharge. For gauged catchments, the mean annual maximum flood discharge is estimated from the measured streamflow series. For ungauged catchments, the mean annual maximum flood is estimated by linear regression using physiographic and climatic catchment descriptors. Then, the method is evaluated for ten catchments located in the Tröllaskagi region and in the West-fjords using annual maximum instantaneous (D=0) and daily (D=24h) streamflow series. The results indicate that the method looks promising for the estimation of the T-year flood peak discharge and the associated confidence interval, along river channels, as part of the design of bridges or dams for instance and in other hydrological applications such as reservoir management and analyses of dam safety. This general methodology should be further developed and also tested in other regions.

7

1 Introduction

Various water resource applications require the calculation of the so-called T-year flood peak discharge, *i.e.* the flood peak magnitude with a return period of T-years or flood magnitude observed once every T-years on average. This information is for instance needed for the design of bridges and dams and in hydrological applications such as reservoir management and analyses of dam safety.

Often, information about flood statistics is required at locations where measured streamflow series are either not long enough to allow for a robust calculation of the flood frequency distribution and the estimation of long return periods or where no data are available at all. Improper understanding of the probabilistic behaviour of floods at the location of interest may have a serious impact on the project construction cost and the structure life time.

One way of estimating design floods, especially in urban hydrology, is by the application of the rational formula which converts extreme precipitation statistics into extreme flood statistics (see for instance Elíasson, 1999, 2002). Another way to derive streamflow statistics is by distributed hydrological modeling. A distributed hydrological model is calibrated for a gauged catchment and used to simulate the discharge series anywhere along the river channels of that catchment and streamflow statistics are extracted. Such a procedure was adopted by Þórarinsdóttir (2012) to calculate flow-duration-curves and thereafter the hydropower potential every 25 meters along the river channels of three catchments in Northern Iceland, with the WaSiM-ETH distributed hydrological model used at the Icelandic Meteorological Office (IMO). Similarly, Atladóttir *et al.*(2011) estimated the T-year flood for ungauged catchments in the West-fjords using the same WaSiM-ETH model. The results indicated that the quality of the estimated T-year flood was strongly dependent on i) the capacity of the hydrological model to properly simulate extreme floods which turned out to be more difficult in winter than during other seasons for the tested catchments, and ii) the physiographic and hydrologic similarities between calibrated and uncalibrated catchments, meaning that rescaling of various model parameters might be necessary, especially if the drainage areas of calibrated and uncalibrated catchments are very different. Despite the intrinsic advantages of the hydrological model, another limitation is related to the temporal resolution (D) of the simulated streamflow series (D=24h), imposed by the available input meteorological information used to run the model. In practise, some sort of downscaling would be needed for applications requiring sub-daily T-year flood estimates.

In this study, a statistical approach, the so-called index flood method (Dalrymple, 1960), is developed for estimating the T-year flood at poorly gauged and ungauged natural catchments (no regulation and no water extraction), using extreme flood statistics available at gauged catchments. Such an approach is widely used by hydrologists and engineers for design flood estimation (see for instance Stedinger *et al.*, 1992; GREHYS, 1996). The advantage of this method is that it works directly with the quantity of interest, the discharge, and not with an indirect quantity like precipitation. The main limitation is related to the available number of gauged catchments for the development of the method which is usually low compared to the available number of raingauge stations. A poorly gauged catchment can be defined as a catchment with only a few years of streamflow measurements or a catchment with a number of years of measurements substantially lower than the considered return period T. An ungauged catchment is defined as a

catchment without streamflow measurement at the point of interest, *i.e.* that a catchment with a gauging station is considered ungauged anywhere upstream of that station.

This report is organized as follows. Section 2 presents the data used in the study. Section 3 describes the index flood method and Section 4 presents its application to the estimation of instantaneous and daily T-year flood peaks. A particular attention is given to the estimation of the uncertainty associated with the quantile estimates, expressed in the form of a confidence interval. Finally, Section 5 concludes this report.

2   Data

2.1   River basins

A set of ten river catchments has been selected for this study. Five of them are located in Northern Iceland, in the Tröllaskagi region and its surroundings (Region 1) and the other five in North-western Iceland, mainly in the West-fjords (Region 2). The location of catchments is shown in Fig. 1 with the topographic map and in Fig. 2 with a mean annual precipitation map (Crochet *et al.*, 2007). These two regions are characterised by complex topography and consequently by large precipitation variability. Table 1 summarizes the main physiographic and climatic characteristics. The drainage of the catchment area varies from 37 km^2 for the smallest to 1096 km^2 for the largest. The mean altitude varies from 403 m a.s.l to 934 m a.s.l with large variations within each catchment. As a consequence of that, the precipitation climatology is also quite variable, the annual average varies between 813 mm and 3018 mm over the catchments.

Gauging station	Name	Area (km^2)	Mean elevation (m a.s.l)	Minimum elevation (m a.s.l)	Maximum elevation (m a.s.l)	Mean slope (%)	Precipitation (1971-2000) (mm)
VHM-10	Svartá	398	535	67	894	14	813
VHM-12	Haukadalsá	167	404	54	786	21	1773
VHM-198	Hvalá	195	403	89	576	6	1971
VHM-19	Dynjandisá	37	529	296	689	10	3018
VHM-200	Fnjóská	1096	715	79	1081	17	1312
VHM-204	Vatnsdalsá	103	456	34	762	13	2937
VHM-38	Þverá	43	427	106	521	7	1761
VHM-51	Hjaltadalsá	296	730	78	1265	32	1711
VHM-92	Bægisá	39	934	254	1304	41	1928
VHM-45	Vatnsdalsá	456	553	121	899	4.4	846

Table 1. Main characteristics of river basins.
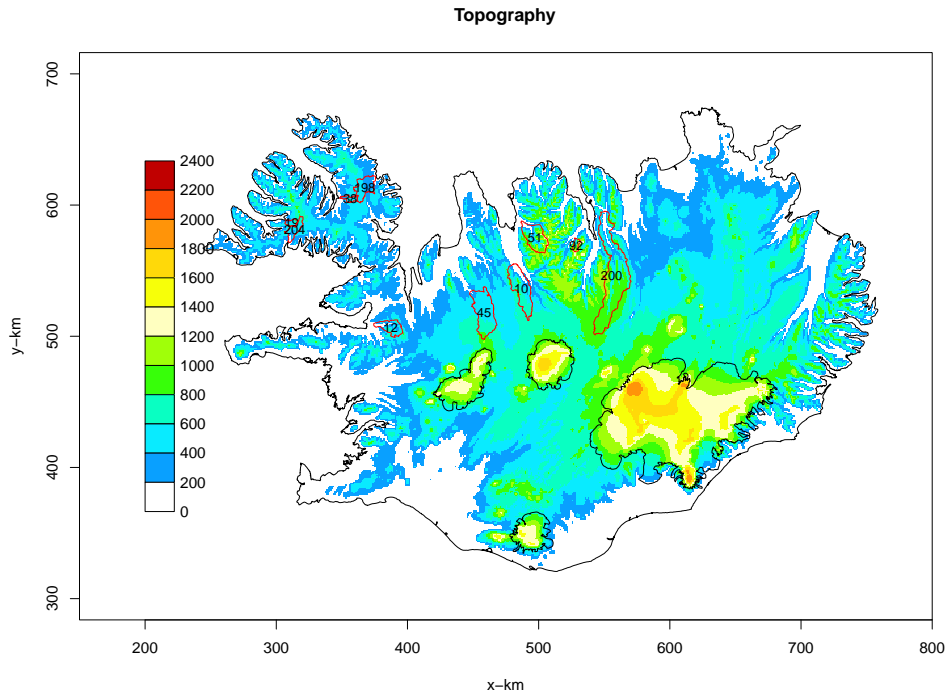
Topography

Figure 1. Topography (m a.s.l) and location of catchments.

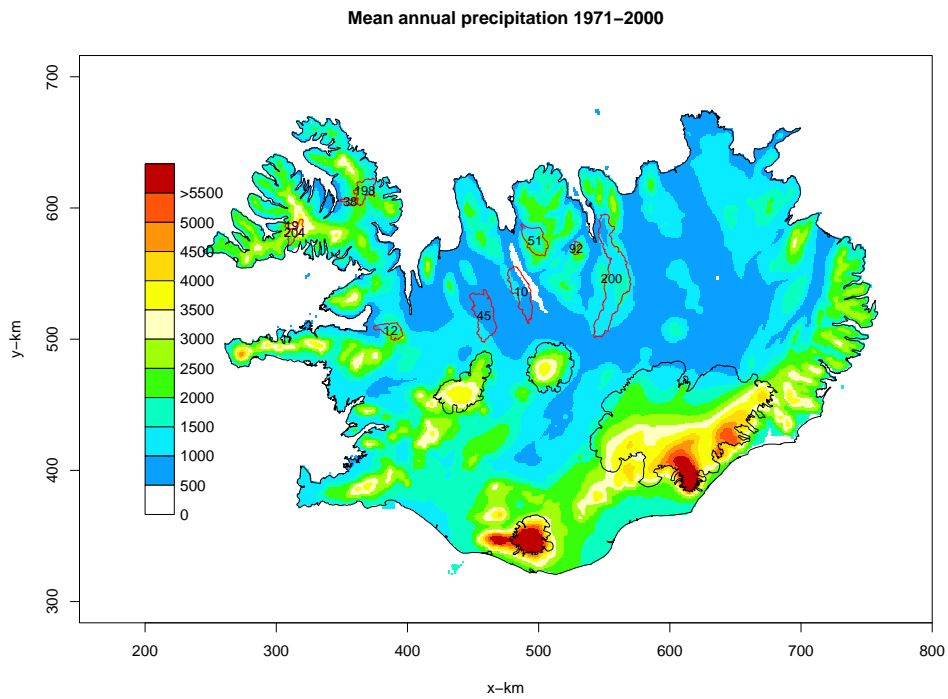**Mean annual precipitation 1971–2000**

Figure 2. Mean annual precipitation (mm) for the standard period 1971–2000 and location of catchments.

10

2.2 Streamflow data

Daily discharge series and monthly maximum instantaneous discharge series were used in this study. Figure 3 presents the long-term averaged daily hydrographs for the hydrological year (1st of September to 31st of August). One can see that most catchments have a well defined seasonality with a low discharge in winter and a high discharge in spring during snowmelt. The timing of the snowmelt peak varies from catchment to catchment and depends on the altitude distribution. A secondary peak is also observed at some catchments between September and October and corresponds to heavy precipitation in autumn. An interesting comparison can be made between VHM-19 and VHM-38. These two catchments are close to each other and have very similar drainage areas but slightly different average altitudes and very different precipitation climatology (see Table 1). The long-term hydrographs indicate that the winter flow is substantially larger for VHM-19 than VHM-38 most likely because of the difference in the precipitation climatology which impacts on groundwater flow. However, the hydrographs are very similar during the spring season, in relation to the snowpack melting, triggered by temperature, which is the main flood-generating mechanism during this season. So one can expect the snowmelt-tiggered floods to be similar in magnitude but the rainfall-triggered floods in autumn or winter to be larger for VHM-19 than VHM-38.

2.3 Annual maximum flood series

Annual maximum daily flood discharge series were extracted for each hydrological year, and years with more than 120 days of missing data were omitted. Annual maximum instantaneous flood discharge series were extracted from the monthly maxima and years with more than four missing months omitted. Finally, only the longest continuous period with no missing years was selected from the annual maximum series of each basin.

Figures 4 and 5 present the annual maximum daily flood discharge versus time of occurrence within the hydrological year. One can see that the largest catchments have most of their annual maxima in late spring or early summer, during snowmelt, such as VHM-200 and VHM-45, but other catchments have annual maxima either in spring, winter or autumn, depending on the year. Large winter floods are the result of large snowmelt often mixed with heavy rain on frozen ground during the passage of warm spells. The dominating flood-generating mechanisms (snowmelt or rain) depend on various factors such as the presence of frozen ground, the catchment size and elevation distribution and the precipitation climatology, among others.
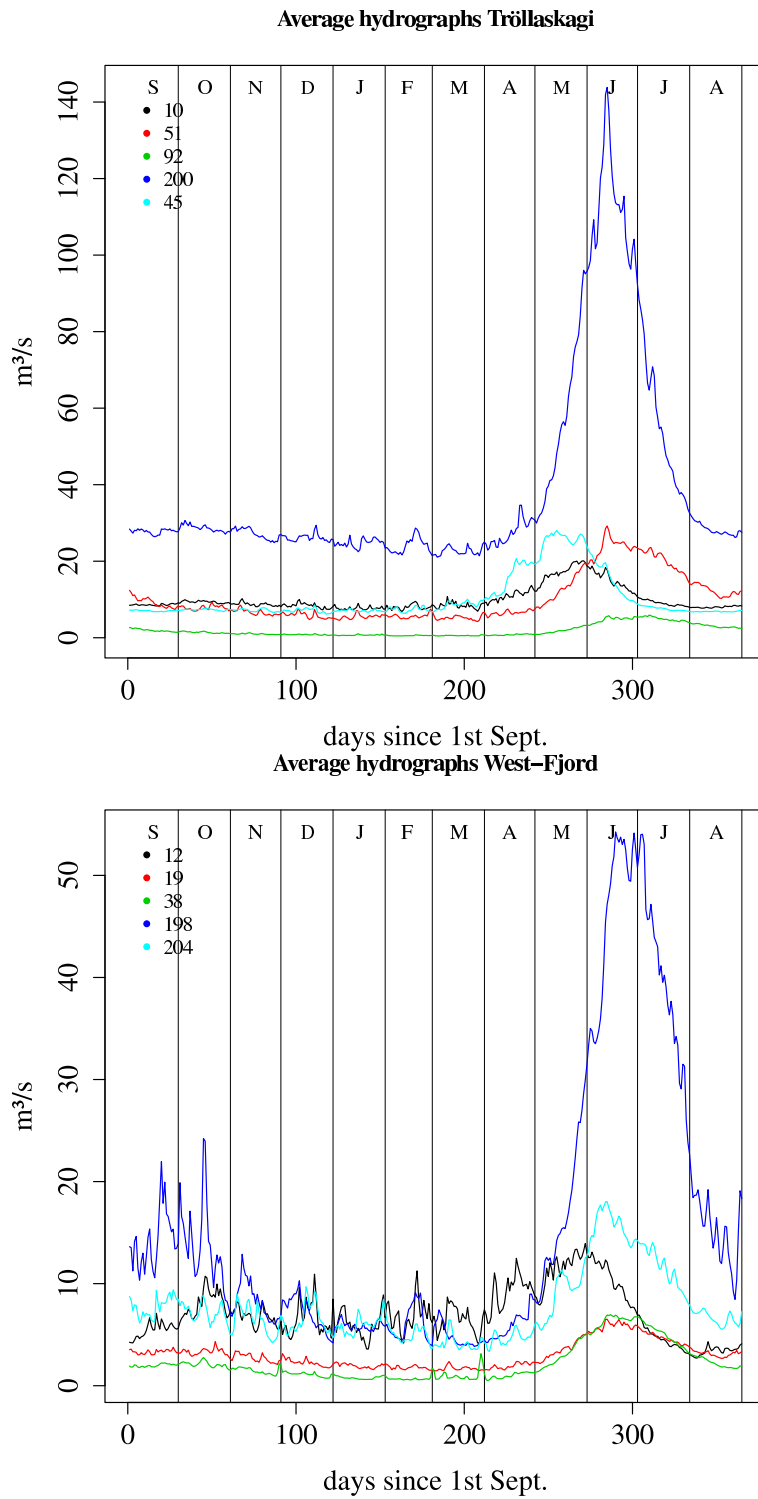
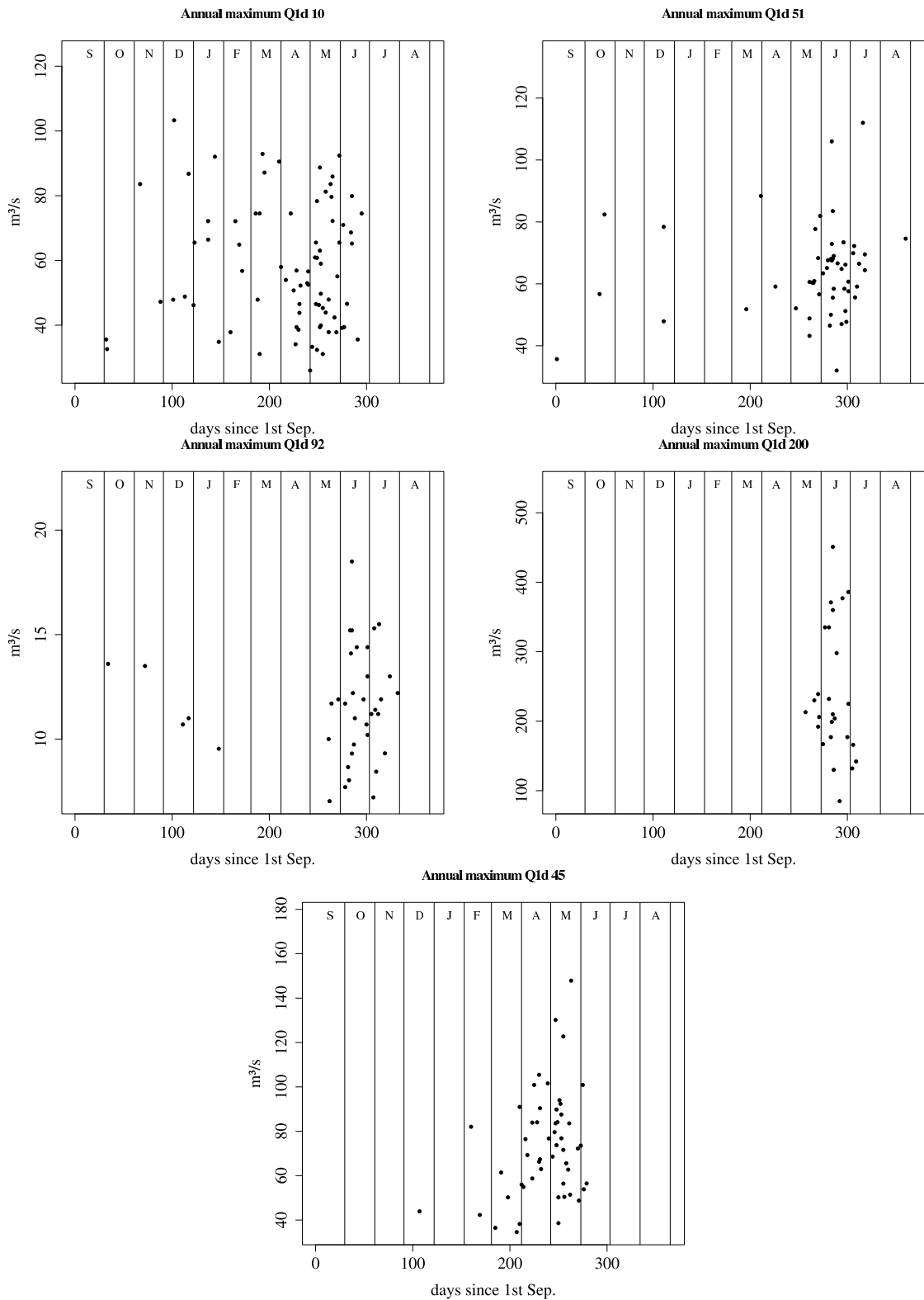Figure 3. Mean daily hydrographs in Region 1 (top) and Region 2 (bottom).

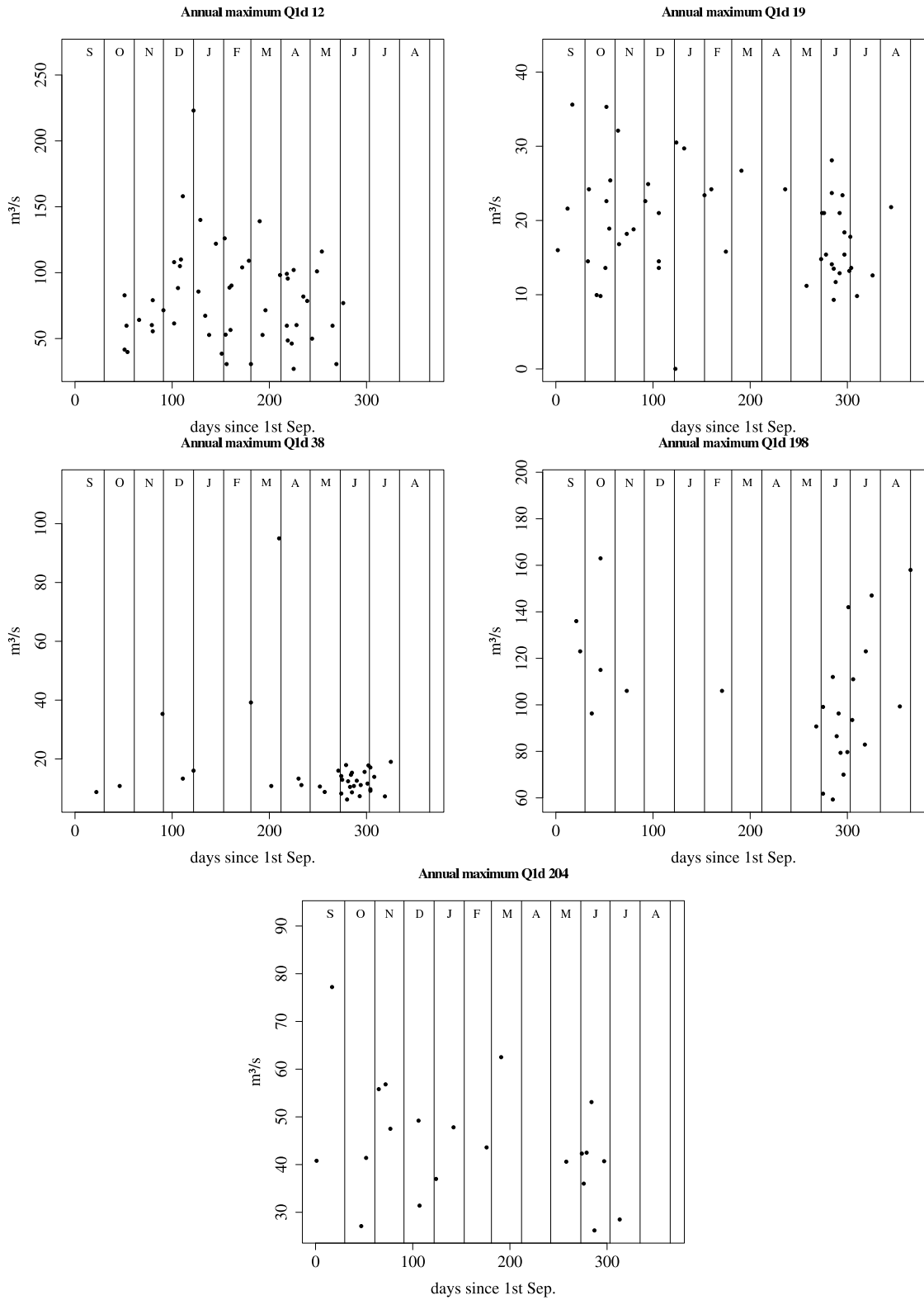*Figure 4. Annual maximum daily flood versus time of occurrence within the hydrological year for Region 1.*

Annual maximum Q1d 12

Annual maximum Q1d 19

Annual maximum Q1d 38

Annual maximum Q1d 198

Annual maximum Q1d 204

Figure 5. Annual maximum daily flood versus time of occurrence within the hydrological year for Region 2.

14

3 Regional flood frequency analysis

3.1 General methodology

The index flood method is a technique developed for estimating the flood frequency distribution at poorly gauged and ungauged catchments. This is performed by scaling a regional flood frequency distribution by the so-called index flood of the catchment, Q_{index}:

$$\widehat{Q}_i(T) = q_R(T)Q_{index}. \tag{1}$$

With $\widehat{Q}_i(T)$ representing the estimated T-year flood peak discharge for a given catchment i and $q_R(T)$ the dimensionless regional T-year flood also called growth factor, representative of a region. The regional growth factor is estimated by pooling together the normalized flood samples of a group of homogeneous gauged catchments, $q_i(j)$:

$$q_i(j) = Q_i(j)/Q_{index}. \tag{2}$$

Where $Q_i(j)$ is the observed maximum flood for gauged catchment i and year j. The underlying assumption is that the normalized probability distribution functions $q_i(T)$, derived from the normalized flood samples at different locations within a "homogeneous region", are identical. Generally, the mean or the median of the annual maximum flood discharge is used as the index flood or scaling factor. In this study, the mean annual maximum flood will be used:

$$Q_{index} = E[Q_i]. \tag{3}$$

For gauged catchments, the mean annual maximum flood can directly be reasonably estimated from the measured flood series, even if the series is short:

$$\widehat{E[Q_i]} = \frac{1}{n}\sum_{j=1}^{n} Q_i(j) \tag{4}$$

For ungauged catchments, the mean annual maximum flood is indirectly estimated, usually with a power-form relationship using physiographic and climatic catchment descriptors, x_k, such as the drainage area, slope, altitude, mean annual precipitation, to name a few:

$$\widehat{E[Q_i]} = a_0 x_1^{a_1} x_2^{a_2} x_3^{a_3} ... x_l^{a_l}. \tag{5}$$

The model parameters a_k can be estimated by multiple linear regression after logarithmic transformation or by non-linear regression (see for instance Grover *et al.*, 2002).

3.2 Flood probability distribution function and parameter estimation methods

The Generalized Extreme Value (GEV) distribution (Jenkinson, 1955) is adopted in this study to model the flood frequency curve of both scaled and unscaled flood series, based on annual maximum flood series. This model is very flexible and is widely used in flood studies. The Cumulative Distribution Function (CDF) for the GEV distribution is:

$$G(q) = \text{Prob}(Q \le q) = \begin{cases} \exp[-(1-\kappa(\frac{q-\varepsilon}{\alpha}))^{1/\kappa}] & \text{if } \kappa \ne 0 \\ \exp[-\exp(-\frac{q-\varepsilon}{\alpha})] & \text{if } \kappa = 0 \end{cases} \tag{6}$$

where Q is the random variable, q a possible value of Q, κ is the shape parameter, ε the location parameter and α the scale parameter. The GEV distribution combines into a single form the three types of limiting distributions for extreme values. Extreme value distribution Type 1 ($\kappa=0$), Type 2 ($\kappa<0$) and Type 3 ($\kappa>0$), respectively. The case with $\kappa=0$ corresponds to the Gumbel distribution. The p-th quantile which is the value q_p with cumulative probability p, ($G(q_p) = \text{Prob}(Q \le q_p) = p$), is estimated as follows:

$$\widehat{q_p} = \begin{cases} \varepsilon + \frac{\alpha}{\kappa}(1 - [-\ln(p)]^\kappa) & \text{if } \kappa \ne 0 \\ \varepsilon - \alpha\ln(-\ln(p)) & \text{if } \kappa = 0 \end{cases} \tag{7}$$

The p-th quantile is associated to the return period $T = 1/(1-p)$ and can also be written as follows:

$$\widehat{q}(T) = \begin{cases} \varepsilon + \frac{\alpha}{\kappa}(1 - [-\ln(1-1/T)]^\kappa) & \text{if } \kappa \ne 0 \\ \varepsilon - \alpha\ln(-\ln(1-1/T)) & \text{if } \kappa = 0 \end{cases} \tag{8}$$

Several approaches are available for estimating the parameters of the GEV distribution, such as the Maximum Likelihood (ML) and the Probability Weigthed Moments (PWM) or the equivalent L-moments (LMOM). According to Hosking *et al.*(1985a), the PWM is more robust than the ML method for small samples, which is the case here and therefore the PWM method will be adopted in this study.

3.3 Regional growth factor

The regional growth factor, $q_R(T)$, will be estimated in this study with the GEV/PWM regionalization algorithm proposed by Hosking *et al.*(1985b). First, the GEV distribution of the annual maximum flood is estimated at each gauged site, i, belonging to a homogeneous region of N sites, by estimating the PWM, $\hat{\beta}_r^i$, ($r=0,1,2$), as defined in Hosking *et al.*(1985a). These PWM are then scaled by $\hat{\beta}_0^i$, the sample mean, to obtain for each site the quantities $\hat{t}_1^i = \hat{\beta}_1^i/\hat{\beta}_0^i$ and $\hat{t}_2^i = \hat{\beta}_2^i/\hat{\beta}_0^i$. Then, the regional estimators $\hat{t}_j^R = \sum_{i=1}^N \hat{t}_j^i n_i / \sum_{i=1}^N n_i$, ($j=1,2$), are calculated, where n_i represents the sample size at site i. Finally, the regional PWM are derived by setting $\hat{\beta}_0^R = 1$, $\hat{\beta}_1^R = \hat{t}_1^R$ and $\hat{\beta}_2^R = \hat{t}_2^R$ and the parameters κ_R, ε_R and α_R of the regional GEV distribution, or regional growth curve, are estimated. Finally, the estimated flood quantile $\widehat{Q}_i(T)$ at a given site i, is calculated with Eq. (1). The index flood Q_{index} is calculated either by Eq. (4) or Eq. (5) and $\hat{q}_R(T)$ given by:

$$\widehat{q}_R(T) = \begin{cases} \varepsilon_R + \frac{\alpha_R}{\kappa_R}(1 - [-\ln(1-1/T)]^{\kappa_R}) & \text{if } \kappa_R \neq 0 \\ \varepsilon_R - \alpha_R \ln(-\ln(1-1/T)) & \text{if } \kappa_R = 0 \end{cases} \tag{9}$$

3.4 Confidence intervals for quantiles

Estimating the uncertainty associated to the quantile $\widehat{Q}_i(T)$ is a very important step in any flood study. This uncertainty is usually expressed in form of a confidence interval. The upper and lower bounds of the $100(1-\theta)\%$ confidence interval of $\widehat{Q}_i(T)$ are given by:

$$\widehat{Q}_i(T) \pm z_{1-\theta/2}\sqrt{\text{Var}\{\widehat{Q}_i(T)\}} \tag{10}$$

where $z_{1-\theta/2}$ is the upper point of the standard normal distribution exceeded with probability $\theta/2$ and the variance of the T-year flood at site i is estimated by:

$$\text{Var}\{\widehat{Q}_i(T)\} = \text{Var}\{\widehat{q}_R(T)\}\widehat{E[Q_i]}^2 + \text{Var}\{\widehat{E[Q_i]}\}E[\widehat{q}_R(T)]^2 + 2\widehat{E[Q_i]}E[\widehat{q}_R(T)]\text{Cov}\{\widehat{E[Q_i]}, \widehat{q}_R(T)\} \tag{11}$$

With $E[\widehat{q}_R(T)] = \widehat{q}_R(T)$ and assuming that $\text{Cov}\{\widehat{E[Q_i]}, \widehat{q}_R(T)\} = 0$.

The asymptotic variance of the three-parameter GEV/PWM p-th quantile (here the regional growth factor $q_R(T)$) can be found in Lu and Stedinger (1992):

$$\begin{aligned} \text{Var}\{\widehat{q}_R(T)\} = {} & (\frac{\partial \widehat{q}_R(T)}{\partial \varepsilon_R})^2 \text{Var}(\varepsilon_R) + (\frac{\partial \widehat{q}_R(T)}{\partial \alpha_R})^2 \text{Var}(\alpha_R) + (\frac{\partial \widehat{q}_R(T)}{\partial \kappa_R})^2 \text{Var}(\kappa_R) \\ & + 2(\frac{\partial \widehat{q}_R(T)}{\partial \varepsilon_R})(\frac{\partial \widehat{q}_R(T)}{\partial \alpha_R})\text{Cov}(\varepsilon_R, \alpha_R) \\ & + 2(\frac{\partial \widehat{q}_R(T)}{\partial \varepsilon_R})(\frac{\partial \widehat{q}_R(T)}{\partial \kappa_R})\text{Cov}(\varepsilon_R, \kappa_R) \\ & + 2(\frac{\partial \widehat{q}_R(T)}{\partial \alpha_R})(\frac{\partial \widehat{q}_R(T)}{\partial \kappa_R})\text{Cov}(\alpha_R, \kappa_R) \end{aligned} \tag{12}$$

where $\widehat{q}_R(T)$ is given by Eq. (9) and

$$\frac{\partial \widehat{q}_R(T)}{\partial \varepsilon_R} = 1 \tag{13}$$

$$\frac{\partial \widehat{q}_R(T)}{\partial \alpha_R} = \frac{1}{\kappa_R}(1 - [-\ln(1-1/T)]^{\kappa_R}) \tag{14}$$

$$\frac{\partial \widehat{q}_R(T)}{\partial \kappa_R} = -\frac{\alpha_R}{\kappa_R^2}(1 - [-\ln(1-1/T)]^{\kappa_R}) - \frac{\alpha_R}{\kappa_R}[-\ln(1-1/T)]^{\kappa_R}\ln(-\ln(1-1/T)) \tag{15}$$

17

and the elements of the asymptotic covariance matrix for the estimators ε_R, α_R and κ_R can be found in Hosking *et al.*(1985a). The formulas for calculating the variance of the mean annual maximum flood, $\text{Var}\{\widehat{E[Q_i]}\}$, when $\widehat{E[Q_i]}$ is estimated either with Eq. (4) or Eq. (5) can be found in books on statistical analysis and regression analysis.

4 Results

For sake of simplicity and because of time limitation and also because few catchments were analysed, the catchments have been split into two groups according to their geographical location. One group in the Tröllaskagi region and surroundings (Region 1: VHM-10, VHM-45, VHM-51, VHM-92, VHM-200) and one group in the West-fjords and surroundings (Region 2: VHM-19, VHM-38, VHM-198, VHM-204, VHM-12). Various methods have been suggested for defining homogeneous groups of catchments based on their physiographic, climatic and geologic characteristics. This will be investigated in a future research.

4.1 Annual maximum instantaneous floods

This section presents the results of the regional flood frequency analysis applied to annual maximum instantaneous ($D = 0$) flood peak discharge.

4.1.1 Regional flood frequency distribution

Figures 6 and 7 present the dimensionless flood CDFs (growth curves) for each catchment and the estimated regional growth curve for the two regions respectively with the estimated 95% confidence interval. One can see, that the growth curves have consistent shapes in Region 2, indicating that the catchments are homogeneous. The growth curves for Region 1 are relatively close to each other, although catchments VHM-51 and VHM-200 are at the border of the estimated 95% confidence interval of the regional growth curve. Several reasons could explain these results. One assumption could be that these two catchments belong to different homogeneous groups and should not be put together. Another assumption is that the different series do not correspond to the same period and some of the descrepancies could result from climate variability. Outliers could also account for some of the discrepancies, especially the largest values, because of uncertainties in the rating curves used to convert extreme water-levels into extreme discharge.

4.1.2 Index flood parameter

The index flood parameter, namely the mean annual maximum instantaneous flood, $E[Q_i]$ (Eq. (3)), was estimated by the sample mean (Eq. (4)) and modeled with Eq. (5), considering the following catchment physiographic parameters: drainage area: A, mean catchment slope: S, mean catchment altitude: Z, catchment perimeter: L, and the following climatic parameters: mean annual area-averaged precipitation for the standard period 1971–2000: P, and mean annual maximum daily surface runoff: Q_S, estimated as the sum of rain and snowmelt calculated from precipitation (Crochet *et al.*, 2007) and temperature (Crochet and Jóhannesson, 2011) and a simple degree day melt model (Crochet, 2010) over the respective catchments. The limited number of catchments under study restricts the number of variables that can be used in the multiple lin-

ear regression model. It was thus decided to use one single explanatory variable by combining several of these parameters together. The six following models have been tested:

$$\widehat{E[Q_i]} = aA^b \tag{16}$$

$$\widehat{E[Q_i]} = a(AP)^b \tag{17}$$

$$\widehat{E[Q_i]} = a(AP/Z)^b \tag{18}$$

$$\widehat{E[Q_i]} = a(AQ)^b \tag{19}$$

$$\widehat{E[Q_i]} = a(A/L)^b \tag{20}$$

$$\widehat{E[Q_i]} = a(AS)^b \tag{21}$$

Figure 8 presents the results for the two regions, using ordinary least squares (OLS) after logarithmic transformation. The coefficient of determination, R^2, is very high in most cases for both regions. It is interesting that when physiographic catchment descriptors only are used, the two regions behave quite differently where as when climatic catchment descriptors are added, the two regions become more alike. A good example is given by the combined use of mean annual precipitation and drainage area for instance (Eq. (17) and Fig. 8, top-right panel) where it is seen that the two regions are almost identical. An interesting example is also seen in Region 2: catchments VHM-19 and VHM-38 have a similar drainage area (see Table 1) but one can see on Fig. 8 (top-left panel) that their mean annual maximum floods are quite different and do not fall near the regression line. Adding another variable such as the mean annual precipitation (top-right panel) or the perimeter (bottom-left panel) improves the relationship. These results also indicate that the best parameter sets to use for estimating the mean annual maximum flood may be different for the different regions. The highest R^2 score is observed with Eqs. (18) and (19) in Region 1 and Eqs. (19) and (20) for Region 2.
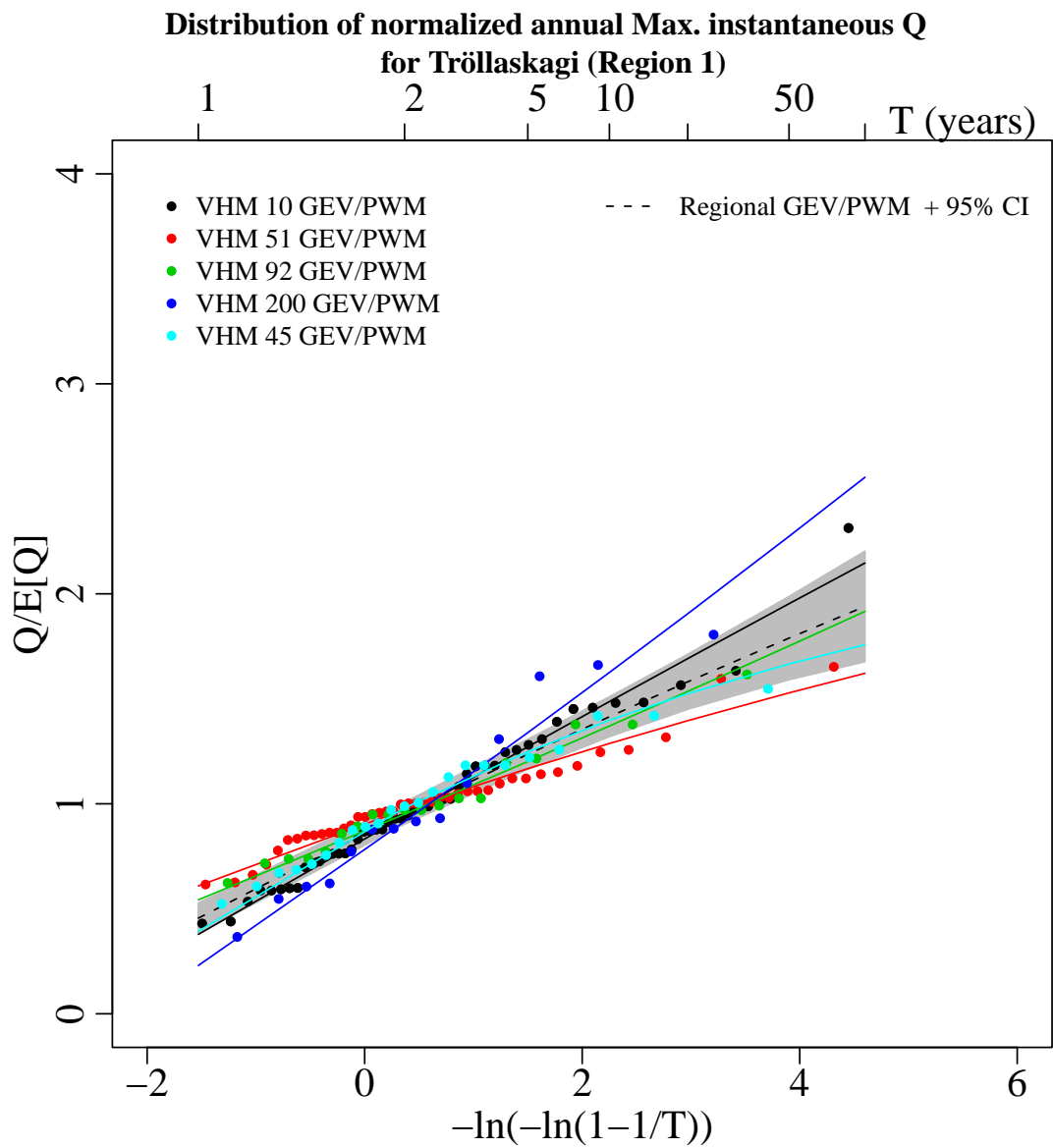
Figure 6. Regional and local dimensionless instantaneous flood CDFs (growth curves) for Region 1. The grey shaded region represents the 95% confidence interval of the regional growth curve.
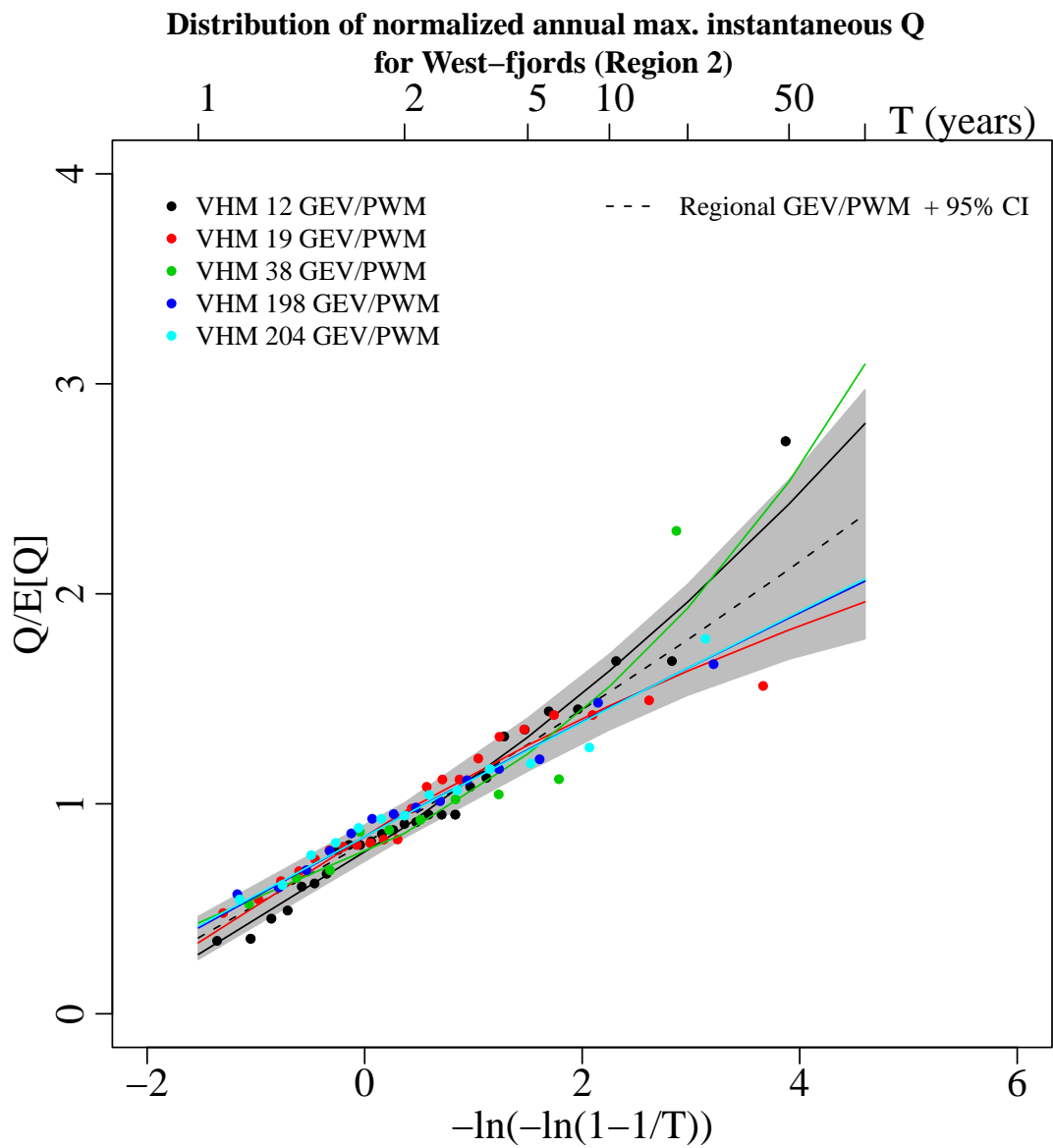
Figure 7. Regional and local dimensionless instantaneous flood CDFs (growth curves) for Region 2. The grey shaded region represents the 95% confidence interval of the regional growth curve.
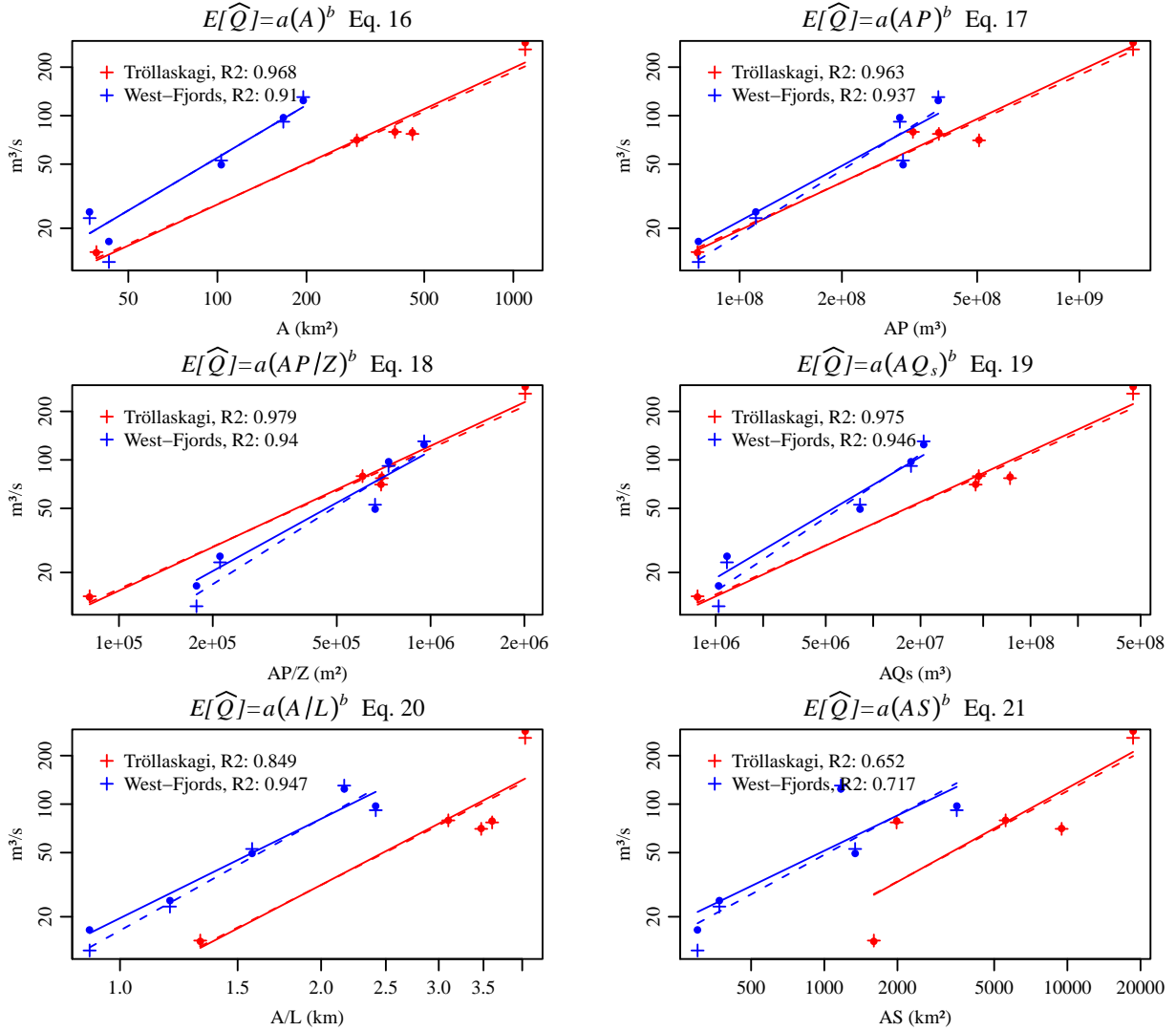
Mean annual maximum instantaneous flood estimation

Figure 8. Mean annual maximum instantaneous flood (index flood) vs. catchment characteristics using the 6 models defined by Eqs. (16)–(21) for Region 1 (red) and Region 2 (blue). The solid lines and open symbols are obtained when $E[Q_i]$ is estimated with all available years and the dashed lines and crosses when $E[Q_i]$ is estimated with the longest continuous series (no missing years within the continuous series).

4.1.3 Flood frequency distribution for ungauged catchments

In order to evaluate the methodology for ungauged catchments and simulate their flood frequency distribution which will then be used to derive the T-year flood peak discharge, the following cross-validation methodology was employed. Each of the 10 catchments was in turn defined as the "ungauged" catchment and its flood data set used as reference only in the validation of the methodology but neither in the calculation of the regional growth curve nor in the calibration of the linear regression models used to estimate the index flood. The regional growth curve and the index flood for each of the ten catchments (five per region) were estimated with Eq. (9) (regional growth curve) and Eqs. (16)–(21) (index flood), using the four other gauged catchments of each region. The flood frequency distribution was then estimated with Eq. (1) and compared to the reference one calculated directly with the observed annual maximum flood data set with the GEV/PWM method. The detailed results of the estimation of the regional growth curves and the calibration of the linear regression models are not given here as they are almost identical to what is shown in Figures 6 to 8, except the data from the catchment under evaluation are not used. The reference and estimated index floods (mean annual maximum instantaneous flood) are presented in Fig. 9.

The reference regional growth curve calculated with all the five catchments of each region and the estimated ones calculated with four catchments at a time are presented in Fig. 10. The estimated flood CDFs of each catchment are presented in Appendix I. Results indicate a fairly consistent estimate of the regional growth curves, meaning that pooling the selected catchments in the same group appears reasonable. The main difficulty is to estimate the index flood of the "ungauged" catchment when its physiographic characteristics are far outside (below or beyond) the observed range of the gauged catchments. In this case, the regression line is extrapolated beyond the observed range and the obtained relationship may not be valid. This is the case in Region 1 for catchment VHM-200, which is by far the largest, and for which the mean annual maximum flood was underestimated by most linear regression models calibrated with the other catchments which are all smaller. Nevertheless, Eq. (17) provided a reasonable estimate, although this model was not the absolutely best one when all five catchments were used together (see Fig. 8). Overall, Fig. 9 indicates that the best model for estimating the index flood at ungauged catchments is Eq. (17) for Region 1 and Eq. (16) for Region 2. These two models are not absolutely best when all five catchments are used (see Fig. 8) but close to the best ones.

Table 2 summarizes the quality of the estimated flood frequency distributions for each catchment measured by the Root Mean Squared Error (RMSE) between reference and estimated quantiles corresponding to the return periods T=1.01, 2, 5, 10, 20, 50 and 100 years. Table 3 summarizes the results for all watersheds. The error depends both on the quality of the index flood estimation and on the regional growth curve. As a consequence, the best results are not systematically obtained with the best index flood, given by the catchment sample mean flood (Eq. (4)), because of compensating errors such as an over- (under-) estimation of the regional growth factor and an under- (over-) estimation of the index flood. However, the dominating source of error when the catchment is considered "ungauged" is usually the quality of the index flood estimation (Eq. 16–21) and the best result is quite often obtained with the regression model giving the best index flood estimate or close to the best one. It is observed that when the index flood at the "ungauged" catchment is estimated with Eqs. (16)–(21), the best results are often obtained with Eq. (16) and Eq. (17) for Region 1 but no method appears as the best one for Region 2.

Overall for both regions, the best results for calculating the flood frequency distribution are obtained when the index flood is estimated with Eq. (17). It is also observed in Appendix I that when the index flood of the catchment is rather well estimated, the estimated quantiles are within the 95% confidence interval of the reference distribution (grey region), and vice-versa, the reference quantiles are within the estimated 95% confidence interval (green dashed lines).

It is also worth mentioning that the 95% confidence interval estimated with the regional growth curve and the observed sample mean (red dashed lines) is often narrower than the one calculated directly with the reference flood sample (grey region), meaning that when the catchment is poorly gauged and a few years only of measurements are available, the use of the regional growth curve combined with the observed index flood of the catchment gives more accurate quantile estimates than those calculated with the observed flood series.

In conclusion, it is important to include a representative panel of catchments during the model development and restrict the use of the method to catchments having physiographic and climatic characteristics within or close to the observed range at the gauged catchments used to build the model. An under- or over-estimation of the catchment index flood may have a strong impact on the estimated flood frequency, even if the regional growth curve is well estimated and representative of the catchment of interest. In practise of course, all the available gauged catchments will be used in the calibration of the regional model and in the case of the two tested regions, the gauged catchments cover a wide range of catchment characteristics.

Gauging station	Ref: $\widehat{E[Q_i]} =$ $\frac{1}{n}\sum_{j=1}^n Q_i(j)$ Eq. (4)	$\widehat{E[Q_i]} =$ aA^b Eq. (16)	$\widehat{E[Q_i]} =$ $a(AP)^b$ Eq. (17)	$\widehat{E[Q_i]} =$ $a(AP/Z)^b$ Eq. (18)	$\widehat{E[Q_i]} =$ $a(AQ_S)^b$ Eq. (19)	$\widehat{E[Q_i]} =$ $a(A/L)^b$ Eq. (20)	$\widehat{E[Q_i]} =$ $a(AS)^b$ Eq. (21)
VHM-10	13.7	8.7 *	42.6	18.9	15	13.8	19.6
VHM-51	18.6	16.6 *	62.8	46.2	29.8	79.2	123
VHM-92	0.75	9.9	6.4 *	8.9	9.7	18	57
VHM-200	97.8	221	112 *	197	208	303	258
VHM-45	8.3	47.9	5.9 *	23.3	42.4	72.1	77.4
VHM-12	29.1	18.9	57.2	47.5	16.7 *	95.6	260
VHM-19	6.3	16.7	3.3 *	8.9	11.8	9.2	3.5
VHM-38	4.5	17.4	3.3	6.2	9.5	3 *	19.7
VHM-198	25.2	20.6 *	37.8	27.9	31.9	58.5	121
VHM-204	9.8	12.3	76.1	57	26.5	5.7 *	28.5

Table 2. Instantaneous flood Quantiles: Root Mean Squared Error for each catchment. The best regression model is highlighted with a *.

Index flood estimation model	$\widehat{E[Q_i]} =$ $\frac{1}{n}\sum_{j=1}^n Q_i(j)$ Eq. (4)	$\widehat{E[Q_i]} =$ aA^b Eq. (16)	$\widehat{E[Q_i]} =$ $a(AP)^b$ Eq. (17)	$\widehat{E[Q_i]} =$ $a(AP/Z)^b$ Eq. (18)	$\widehat{E[Q_i]} =$ $a(AQ_S)^b$ Eq. (19)	$\widehat{E[Q_i]} =$ $a(A/L)^b$ Eq. (20)	$\widehat{E[Q_i]} =$ $a(AS)^b$ Eq (21)
RMSE	34.4	72.9	53.7 *	69.6	69.8	108	132

Table 3. Instantaneous flood quantiles: Root Mean Squared Error over all catchments. The best regression model is highlighted with a *.
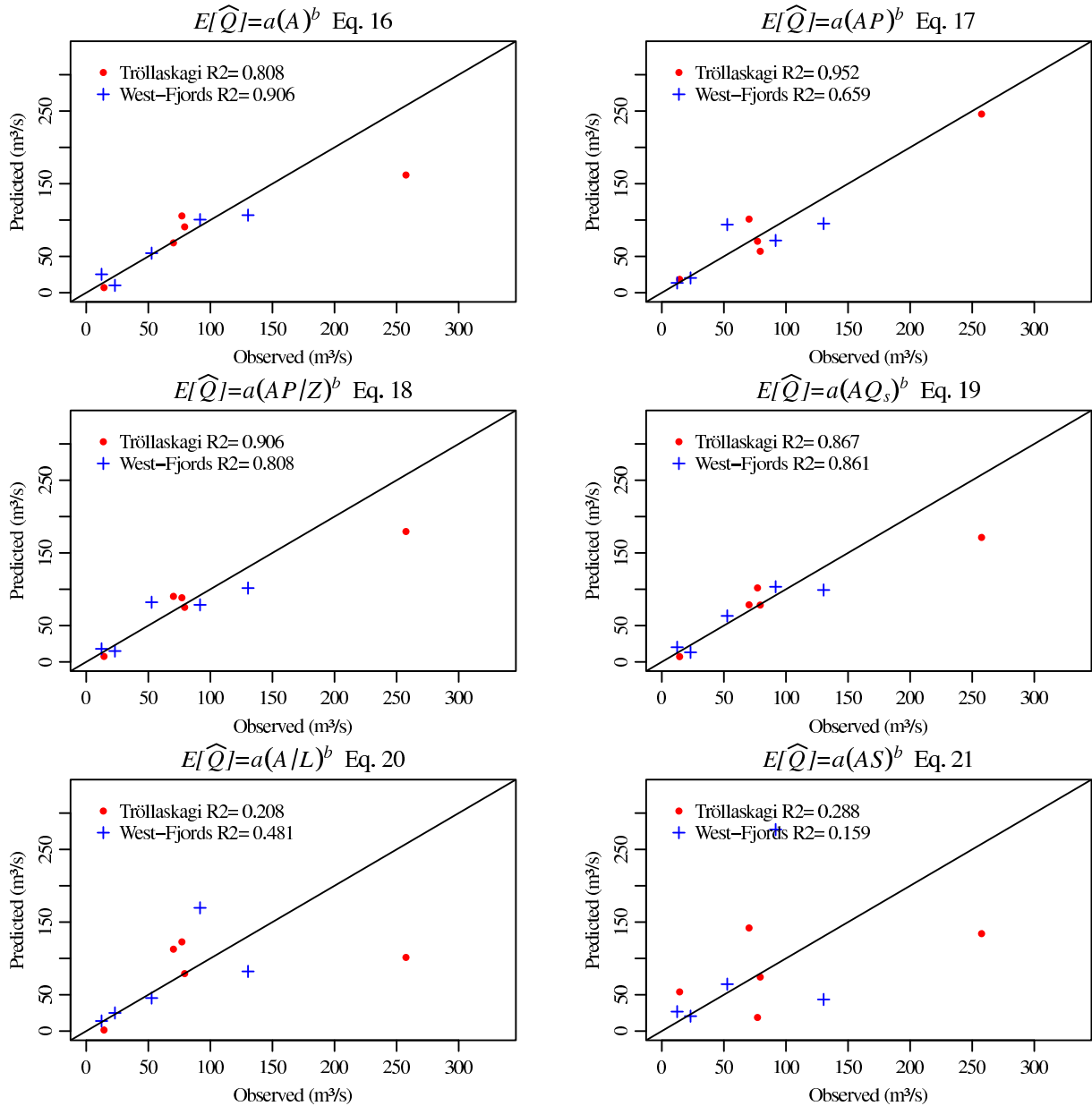
Figure 9. Observed vs. estimated mean annual maximum instantaneous flood at reference catchments assumed "ungauged", using 6 different models (see Eqs. (16–21)). The observed mean for the catchment in question is not used in the calibration of Eqs. (16–21).

26
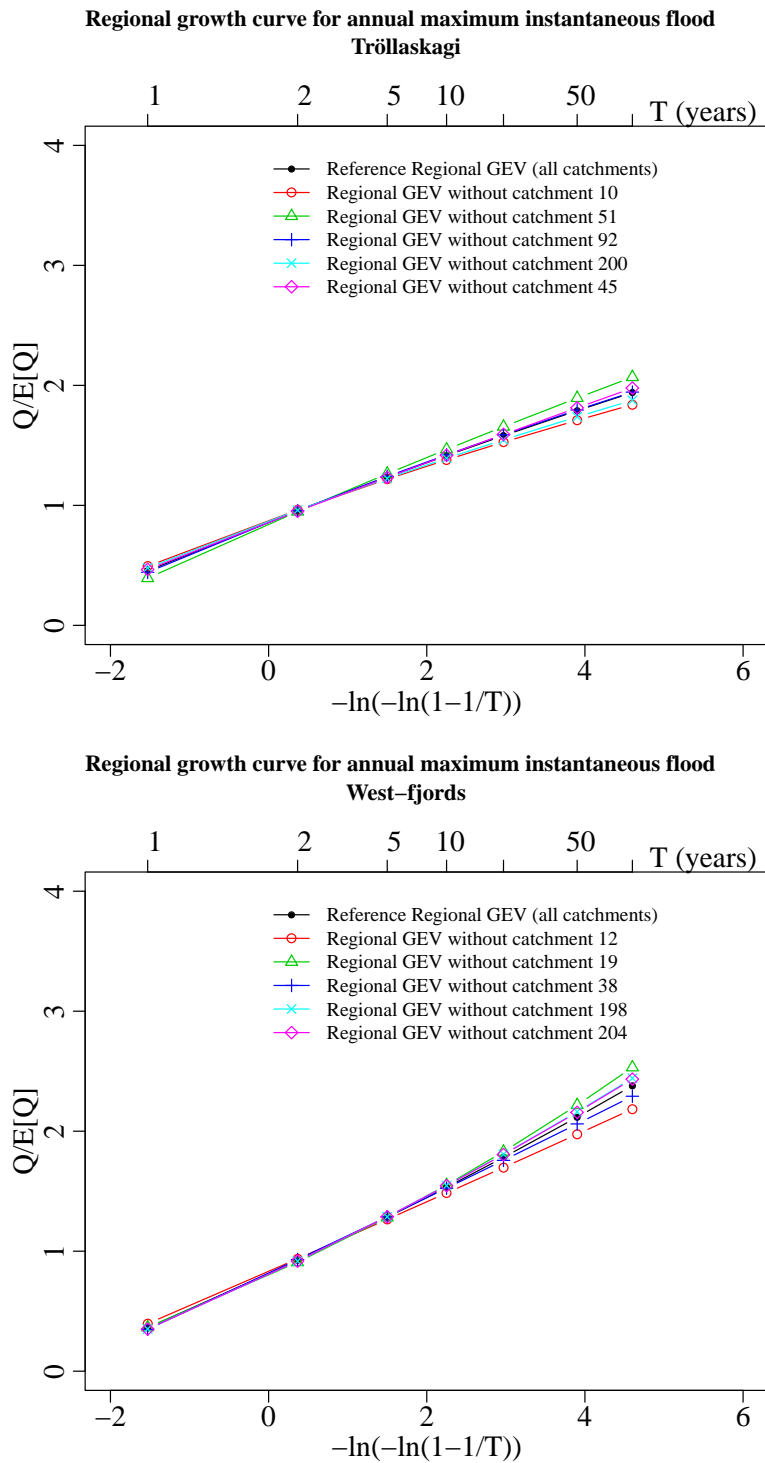
Figure 10. Reference and estimated regional growth curves for annual maximum instantaneous flood. Region 1 (top) and Region 2 (bottom). The reference growth curve is calculated with all 5 catchments of each region and the estimated ones with 4 catchments, by eliminating one at a time.

4.2 Annual maximum daily floods

This section presents the results of the regional flood frequency analysis applied to annual maximum daily ($D = 24h$) flood peak discharge.

4.2.1 Regional flood frequency distribution

Figures 11 and 12 present the dimensionless flood CDFs (growth curves) for each catchment and the estimated regional growth curve for the two regions with the estimated 95% confidence interval. Results are similar to those observed previously with the instantaneous flood peak discharge. Here too, the growth curves of daily flood peak discharge are close to each other in Region 2 and also in Region 1 except for catchments VHM-51 and VHM-200 which are at the border of the estimated 95% confidence interval of the regional growth curve (see comments in section 4-1-1).

4.2.2 Index flood parameter

The index flood parameter was estimated by the mean annual maximum daily flood (Eq. 4) and modeled with Eq. (16)–(21), as for the instantaneous floods. Figure 13 presents the results for the two regions. The coefficient of determination, R^2, is high in most cases for both regions and the results are similar to those observed previously with the mean annual maximum instantaneous flood, so the same comments are valid. Here too, the best parameter sets to use in Eq. (5) for modeling the mean annual maximum flood may be different for different regions. For Region 1, Eqs. (16)–(19) give very high R^2 scores and the best model is given by Eq. (18) while for Region 2, Eq. (20) is best.

4.2.3 Flood frequency distribution for ungauged catchments

In order to evaluate the methodology at ungauged catchments, the same cross-validation methodology used in Section 4-1-3 with instantaneous flood was employed. Four catchments were used to calculate the regional growth curve and estimate the index flood to be used at the fifth catchment considered "ungauged". The reference and estimated index floods are presented in Fig. 14. The reference and estimated regional growth curves calculated without using the catchments under study are presented in Fig. 15. The estimated flood frequency distributions of each catchment are presented in Appendix II. Once more, results indicate a fairly consistent estimation of the regional growth curve, except when catchment VHM-12 is removed. This is because the growth curve of VHM-12 is not bounded and is drawing the high frequencies towards higher values when it is used. This could perhaps indicate that the most extreme values for this catchments are uncertain (due to the possible difficulty in converting extreme water levels into extreme floods with the available rating curves) or that VHM-12 should belong to another group.

As for the instantaneous floods, the main difficulty is to estimate the index flood of the "ungauged" catchment when its physiographic and climatic characteristics are far outside (below or beyond) the observed range at the gauged catchments. The estimated mean annual maximum daily flood at catchment VHM-200, which is by far the largest of Region 1, is underestimated by most linear regression models except by the one defined by Eq. (17) (not shown). In practise of course, all the available catchments will be used in the calibration of the regional model.

Overall, the best index flood estimates are obtained with Eq. (17) for Region 1 and with Eq.

(16) for Region 2. Table 4 summarizes the quality of the estimated flood frequency distributions for each catchment measured by the Root Mean Squared Error (RMSE) between reference and estimated quantiles corresponding to the return periods T=1.01, 2, 5, 10, 20, 50 and 100 years. Table 5 summarizes the results for all watersheds. As mentioned previously, the error depends both on the quality of the index flood estimation and on the regional growth curve. Using the best index flood (calculated with the observed flood sample), does not always guaranty to obtain the best flood frequency distribution if large biases affect the regional growth curve. However, the largest source of error is usually due to the bias in the index flood estimate. The results obtained for each catchment do not point to one single index flood estimation model (Eqs.16–21) better than the others. The overall results however indicate that the index flood calculated with Eq. (17) leads to the best results as for instantaneous flood. Here too, results of Appendix II indicate that when the index flood is rather well estimated, the estimated quantiles are within the 95% confidence interval of the reference distribution and vice-versa, the observed flood quantiles are within the estimated 95% confidence interval.

Gauging station	$\widehat{E[Q_i]} = \frac{1}{n}\sum_{j=1}^{n} Q_i(j)$ Eq. (4)	$\widehat{E[Q_i]} = aA^b$ Eq. (16)	$\widehat{E[Q_i]} = a(AP)^b$ Eq. (17)	$\widehat{E[Q_i]} = a(AP/Z)^b$ Eq. (18)	$\widehat{E[Q_i]} = a(AQ_S)^b$ Eq. (19)	$\widehat{E[Q_i]} = a(A/L)^b$ Eq. (20)	$\widehat{E[Q_i]} = a(AS)^b$ Eq (21)
VHM-10	6.9	22	20.1	4.6	7.4	8.8	4.3*
VHM-51	16	9.5 *	43.8	30	17	57.9	91
VHM-92	1.8	5.7	6.4	5.6 *	6.1	13	51.2
VHM-200	183	278	174 *	255	265	347	312
VHM-45	7.8	30	14.5	11 *	25.7	51.2	74.6
VHM-12	33.4	29.6	58.7	51.5	26.3	65.9	20.3 *
VHM-19	1.7	17.4	4.7	11.4	13.7	1.8 *	4.9
VHM-38	2.3	21.7	5.9 *	11.9	14.8	6.3	22.6
VHM-198	29.3	16.8	15.2	14.6	14.3 *	28.9	82.2
VHM-204	4	2.7 *	53.7	38	13.7	9.7	15.9

Table 4. Daily flood quantiles: Root Mean Squared Error for each catchment. The best regression model is highlighted with a *.

Index flood estimation model	$\widehat{E[Q_i]} = \frac{1}{n}\sum_{j=1}^{n} Q_i(j)$ Eq. (4)	$\widehat{E[Q_i]} = aA^b$ Eq. (16)	$\widehat{E[Q_i]} = a(AP)^b$ Eq. (17)	$\widehat{E[Q_i]} = a(AP/Z)^b$ Eq. (18)	$\widehat{E[Q_i]} = a(AQ_S)^b$ Eq. (19)	$\widehat{E[Q_i]} = a(A/L)^b$ Eq. (20)	$\widehat{E[Q_i]} = a(AS)^b$ Eq (21)
RMSE	59.9	89.9	62.9 *	84	85.3	115	128

Table 5. Daily flood quantiles: Root Mean Squared Error over all catchments. The best regression model is highlighted with a *.
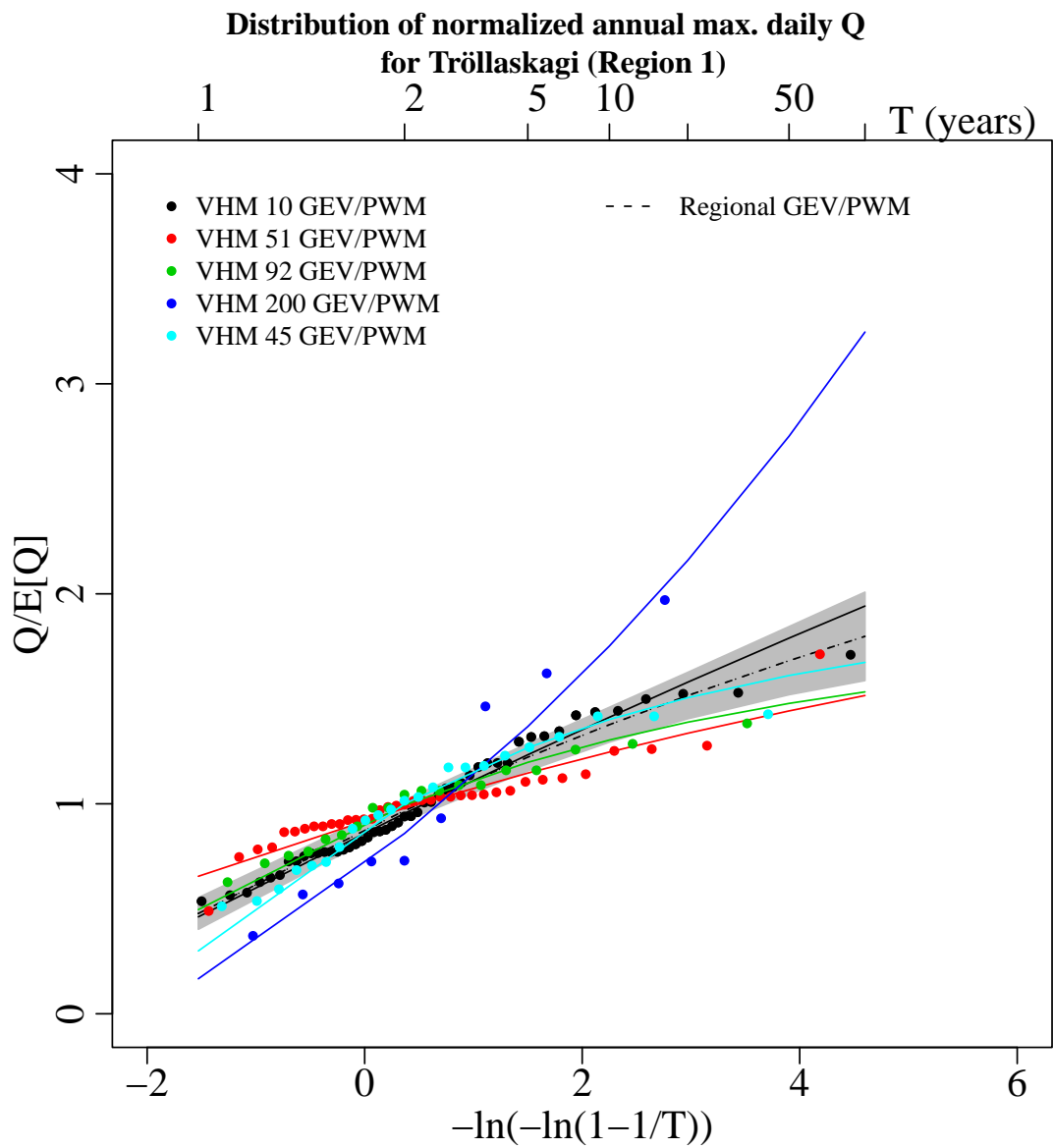
Figure 11. Regional and local dimensionless daily flood CDFs (growth curves) for Region 1. The grey shaded region represents the 95% confidence interval of the regional growth curve.
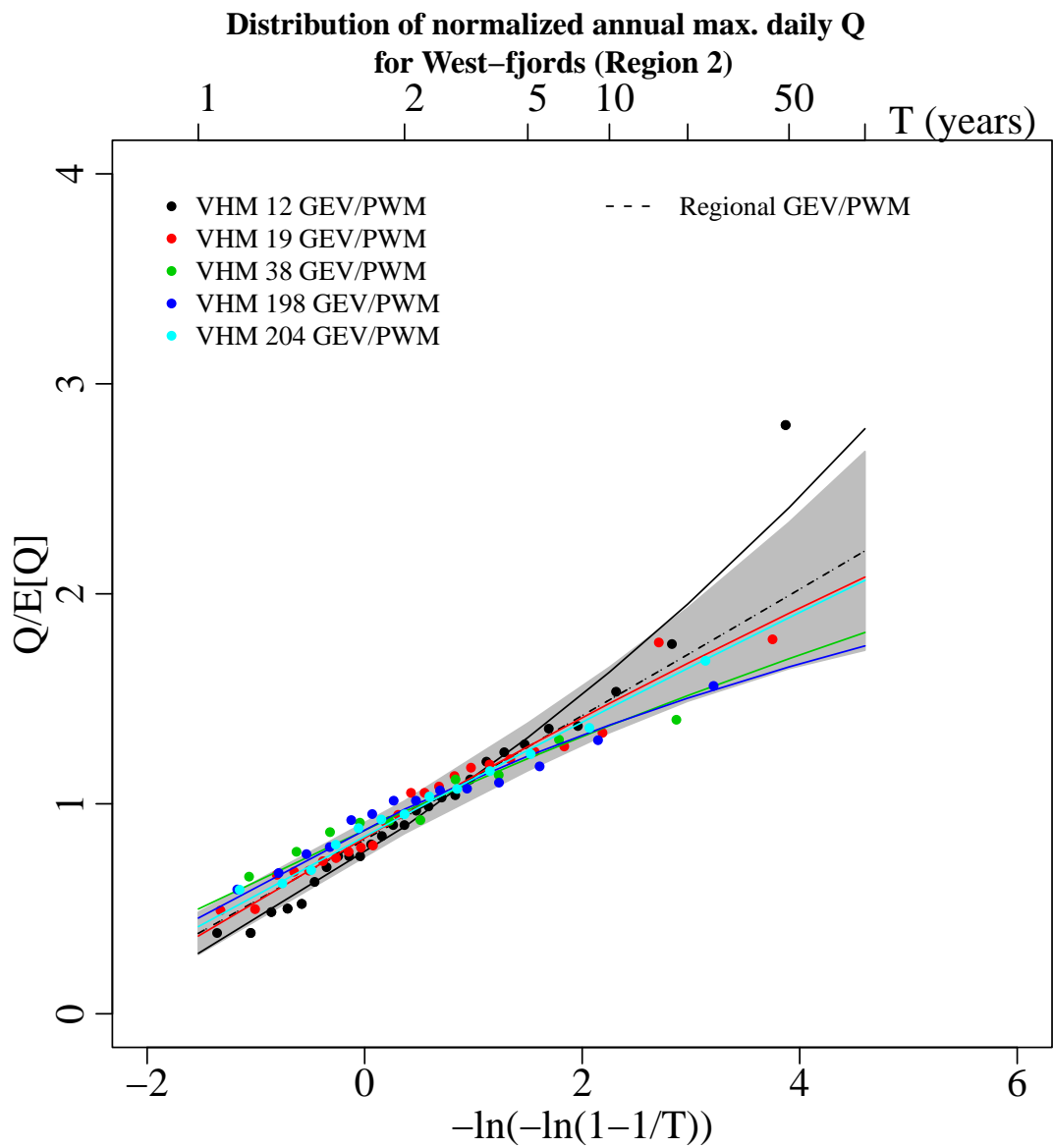
Figure 12. Regional and local dimensionless daily flood CDFs (growth curves) for Region 2. The grey shaded region represents the 95% confidence interval of the regional growth curve.
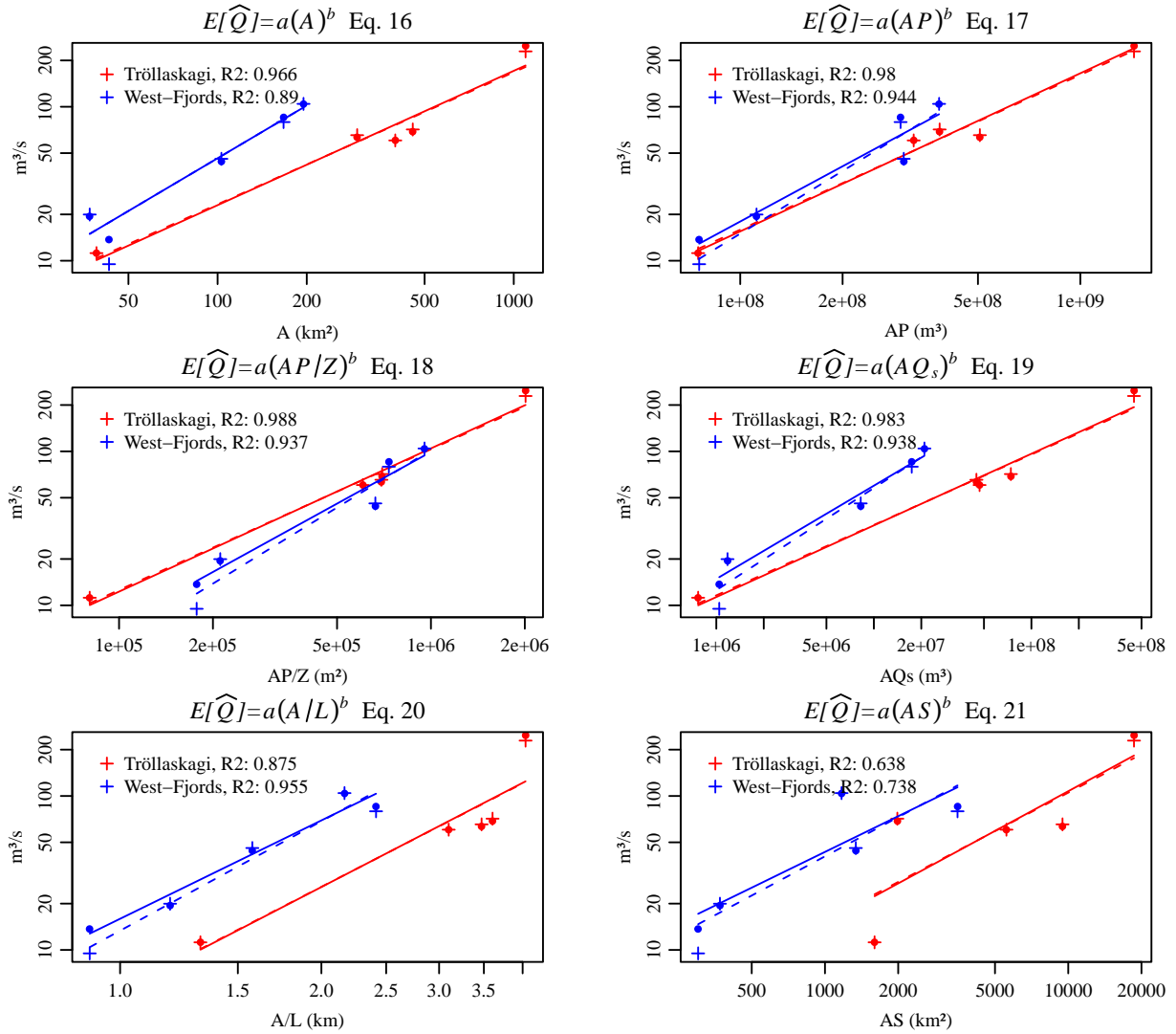
Mean annual maximum daily flood estimation

Figure 13. Mean annual maximum daily flood (index flood) vs. catchment characteristics using the 6 models defined by Eqs. (16)–(21) for Region 1 (red) and Region 2 (blue). The solid lines and open symbols are obtained when $E[Q_i]$ is estimated with all available years and the dashed lines and crosses when $E[Q_i]$ is estimated with the longest continuous series (no missing years).

Mean annual maximum daily flood
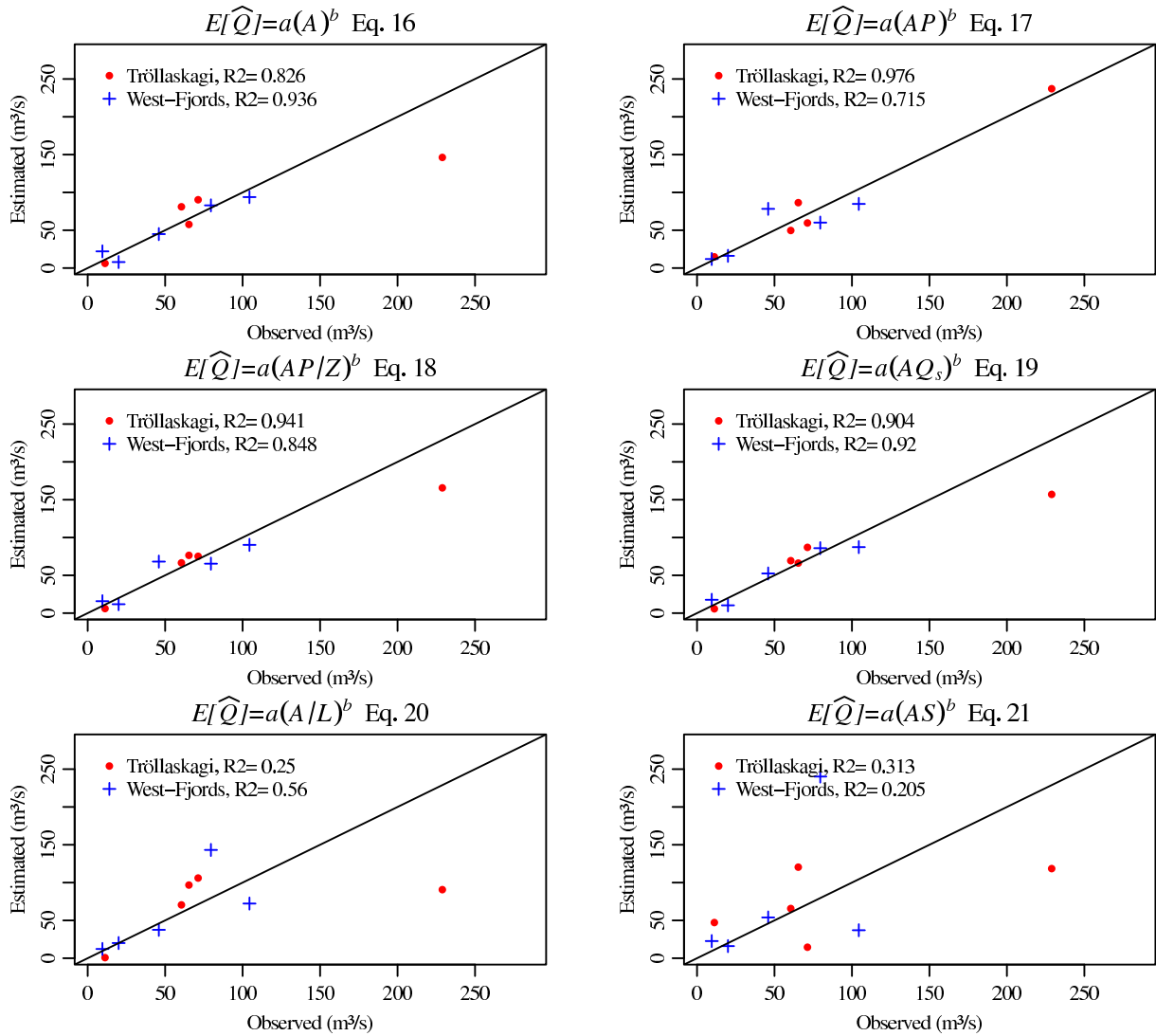
Figure 14. *Observed vs. estimated mean annual maximum daily flood at reference catchments assumed "ungauged", using 6 different models (see Eqs. (16–21)). The observed mean for the catchment in question is not used in the calibration of Eqs. (16–21).*
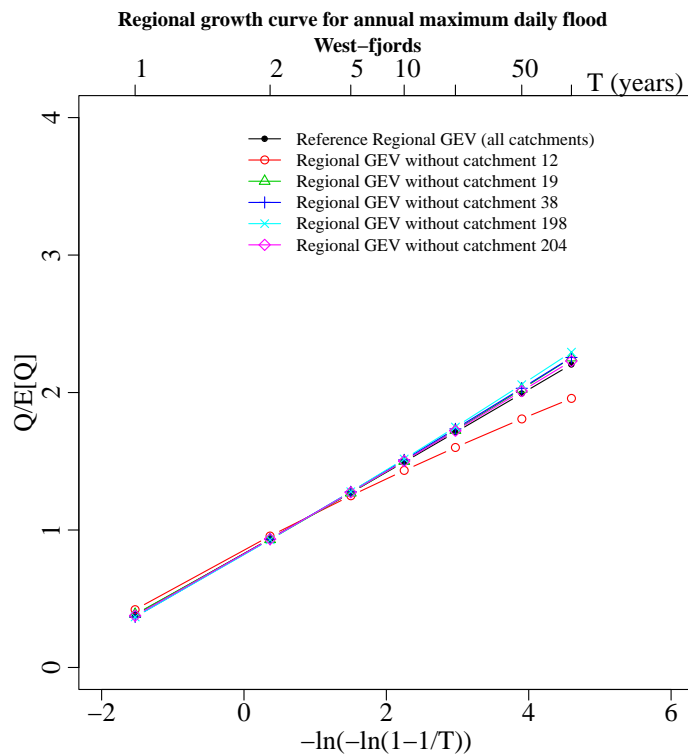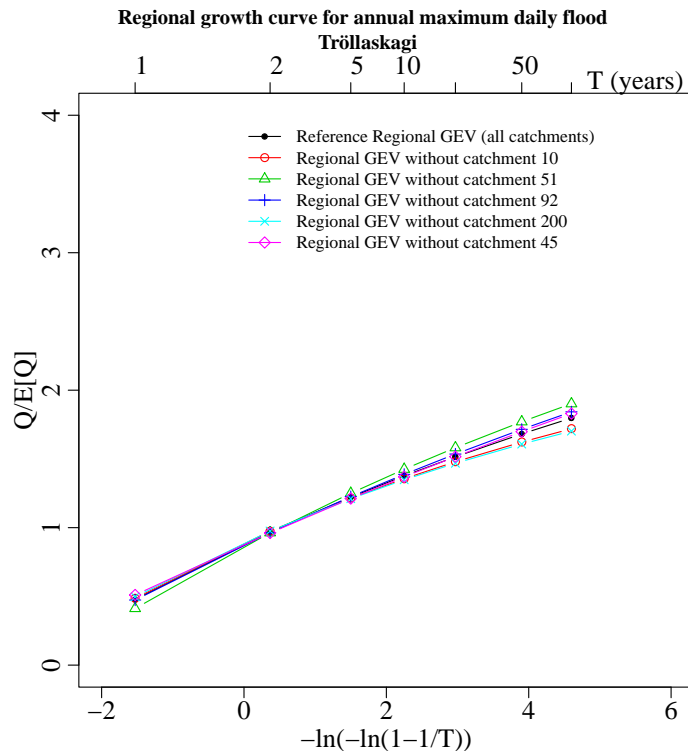
Figure 15. Reference and estimated regional growth curves for annual maximum daily flood. Region 1 (top) and Region 2 (bottom). The reference growth curve is calculated with all 5 catchments of each region and the estimated ones with 4 catchments, by eliminating one at a time.

5   Conclusion and future research

The regional flood frequency analysis developed in this study is shown to be a powerful tool for estimating the flood frequency distribution and calculating the T-year flood and its confidence interval at poorly gauged and ungauged unregulated catchments anywhere along their river channels. Although the regional growth curves calculated in the two tested regions were relatively robust, care must be taken when identifying homogeneous groups and objective strategies for performing this task will be investigated in the future. The main source of error in the method was related to the estimation of the index flood. A poor estimate of the catchment index flood could lead to severe under- or over-estimation of the flood frequency distribution. The relatively small number of gauged catchments used in the study could make the linear regression model uncertain. Another reason for uncertainty could be that all the catchments do not necessarily belong to the same group and putting them together could reduce the quality of the regression model. The selection of the best index flood regression model is as crucial as making the best identification of homogeneous groups as possible. Further testing of additional parameters or combination of parameters in the estimation of the index flood and making use of all possible gauged catchments is planned in the future.

This study focused on annual maximum floods. It was observed that depending on the catchments, these annual maximum floods sometimes took place in the spring, in relation to snowmelt; they took place sometimes in the winter, in relation to snowmelt and heavy rain on frozen ground; they took place sometimes in the autumn during heavy rain. These various types of floods fundamentally differ because the flood generating mechanisms vary. Analysing them separately rather than jointly could improve the overall performance of the method and this will also be considered in future studies.

Finally, this regional flood frequency analysis method could also be combined with the use of the distributed hydrological model WaSiM-ETH used at IMO. WaSiM-ETH could be used on gauged catchments to extract the flood frequency distribution and the index flood at many locations along the river channels to create a much larger number of "gauges" than available in practise. This information could then be used to build a robust regional index flood model to be used at nearby ungauged catchments without having to actually run WaSiM-ETH on these ungauged catchments, since such a run could turn out to be difficult for reasons explained in the Introduction. In a future research, a comparison between these two strategies will be considered.

6   Acknowledgements

7 References

Atladóttir A., P. Crochet, S. Jónsson and H.B. Hróðmarsson. 2011. Mat á flóðagreiningu með rennslisröðum reiknuðum með vatnafræðilíkaninu WaSiM. Frumniðurstöður fyrir vatnasvið á sunnanverðum Vestfjörðum. Icelandic Meteorological Office Rep. 2011-008, 41 pp.

Crochet, P., T. Jóhannesson, T. Jónsson, O. Sigurðsson, H. Björnsson, F. Pálsson and I. Barstad. 2007. Estimating the spatial distribution of precipitation in Iceland using a linear model of orographic precipitation. J. Hydrometeorol., 8, 1285–1306.

Crochet, P., and T. Jóhannesson. 2011. A dataset of daily temperature in Iceland for the period 1949–2010. Jökull, 61, 1–17.

Crochet, P. 2010. Impact of historic climate variations on streamflow characteristics in Icelandic rivers. Proceedings from the conference: Future climate and renewable energy: impacts, risks and adaptation, Oslo, Norway, 31 May - 2 June 2010, 12–13.

Dalrymple, T. 1960. Flood frequency analysis. US Geol. Surv. Water Supply Paper, 1543 A.

Eliasson, J. 1999. Estimation of design floods on basis of M5 values. *Paper intended for presentation at the 12th Northern research basins Symposium and workshp, Reykjavík, Kirkjubæjarklaustur and Höfn, Hornarfjördur, Iceland, August 23-27 1999.*
http://www.hi.is/is/verkfraedi_og_natturuvisindasvid_deildir/
umhverfis_og_byggingarverkfraedideild/rannsoknir/greinar

Eliasson, J. 2002. The rational formula as a linear element in computer runoff models. *Paper accepted at the European Geophysical Conference, April 22-26 2002, Nice, France.*
http://www.hi.is/is/verkfraedi_og_natturuvisindasvid_deildir/
umhverfis_og_byggingarverkfraedideild/rannsoknir/greinar

GREHYS. 1996. Presentation and review of some methods for regional flood frequency analysis. J. Hydrol., 186, 63–84.

Grover, P.L., D.H. Burn, and J.M. Cunderlik. 2002. A comparison of index flood estimation procedures for ungauged catchments. Can. J. Civ. Eng., 29, 731–741.

Hosking, J.R.M, J.R. Wallis, and E.F. Wood. 1985a. Estimation of the generalized extreme-value distribution by the method of the probability-weighted moments. Technometrics, 27(3), 251–261.

Hosking, J.R.M, J.R. Wallis, and E.F. Wood. 1985b. An appraisal of the regional flood frequency procedure in the UK Flood Studies Report. Hydrol. Sci. J., 30, 85–109.

Jenkinson, A.F. 1955. The frequency distribution of the annual maximum (or minimum) of meteorological elements. Quart. J. R. Met. Soc. 81, 158–171.

Lu, L.H. and J.R. Stedinger. 1992. Variance of two- and three-parameter GEV/PWM quantile estimators: formulae, confidence intervals and a comparison. J. Hydrol., 138, 247-267.

Stedinger, J.R., R.M. Vogel and E. Foufoula-Georgiou. 1992. Frequency analysis of extreme events. Handbook of Hydrology, D.R. Maidmment Ed., McGraw-Hill.

Þórarinsdóttir, T. 2012. Development of a methodology for estimation of technical hydropower potential in Iceland using high resolution hydrological modeling. University of Iceland. 106pp.

Appendix I: Observed and estimated flood cumulative distribution functions (CDFs) for annual maximum instantaneous flood using a regional growth curve and 6 different index flood models

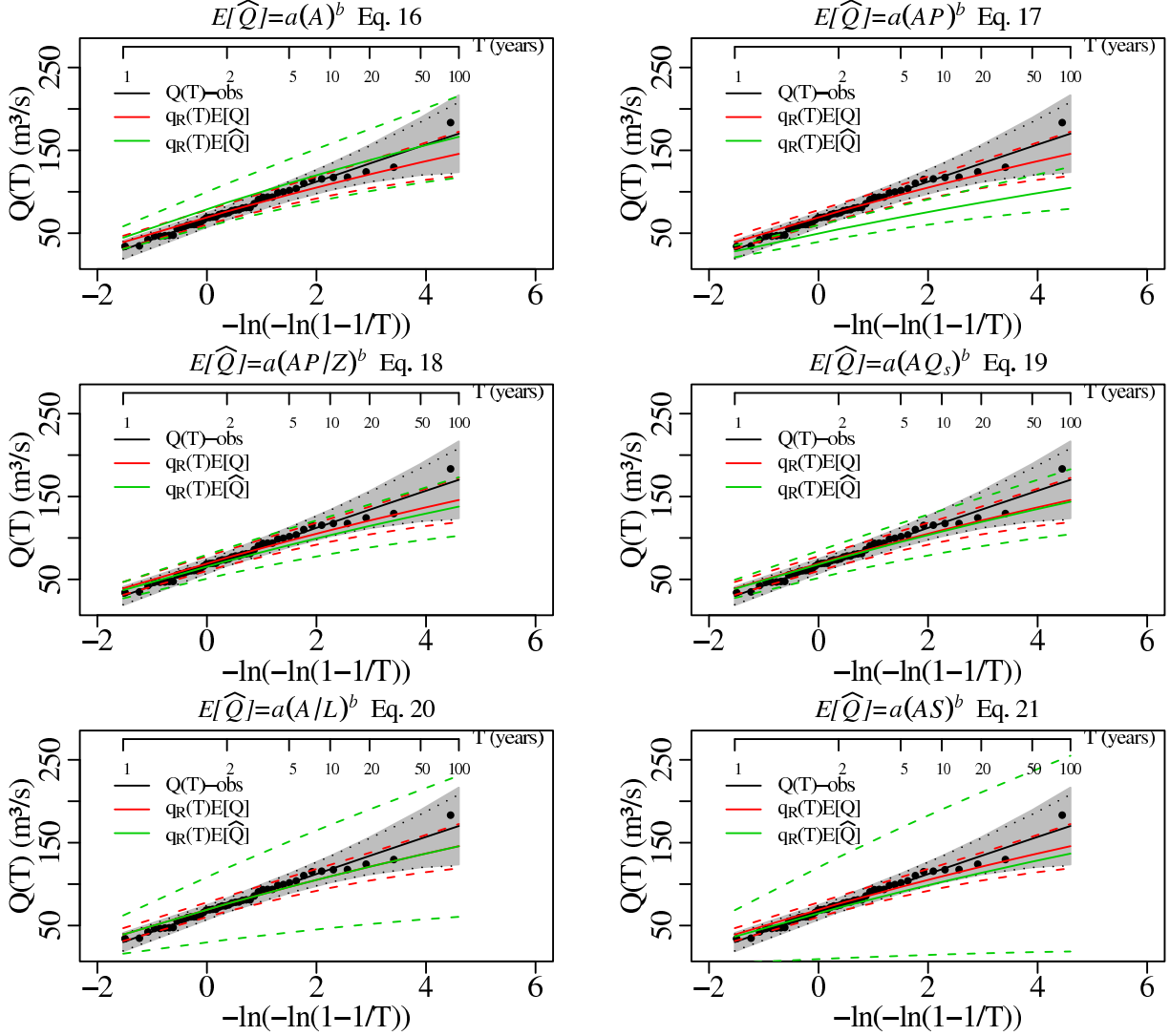**Distribution of annual max. instantaneous Q, VHM 10**

Figure I.1. Observed and estimated flood CDFs for annual maximum instantaneous flood at VHM-10. The solid black line represents the reference GEV/PWM distribution estimated with the observed flood sample, the grey shaded region represents the 95% confidence interval and the dotted black line the 95% bootstrap confidence interval. The solid red line corresponds to the GEV distribution estimated with Eq. (1), by the product of the regional growth curve $q_R(T)$ and an index flood estimated by the observed sample mean $E[\widehat{Q_i}]$ (Eq. 4). The solid green line corresponds to the GEV distribution estimated with Eq. (1), by the product of the regional growth curve $q_R(T)$ and an index flood estimated by the linear model $\widehat{E[Q_i]} = a_0 x_1^{a_1} x_2^{a_2} x_3^{a_3} \dots x_l^{a_l}$ (Eqs. 16–21). The colored dashed lines give their respective 95% confidence intervals.

Distribution of annual max. instantaneous Q, VHM 51

Figure I.2. Observed and estimated flood CDFs for annual maximum instantaneous flood at VHM-51. See caption of Fig. I.1.
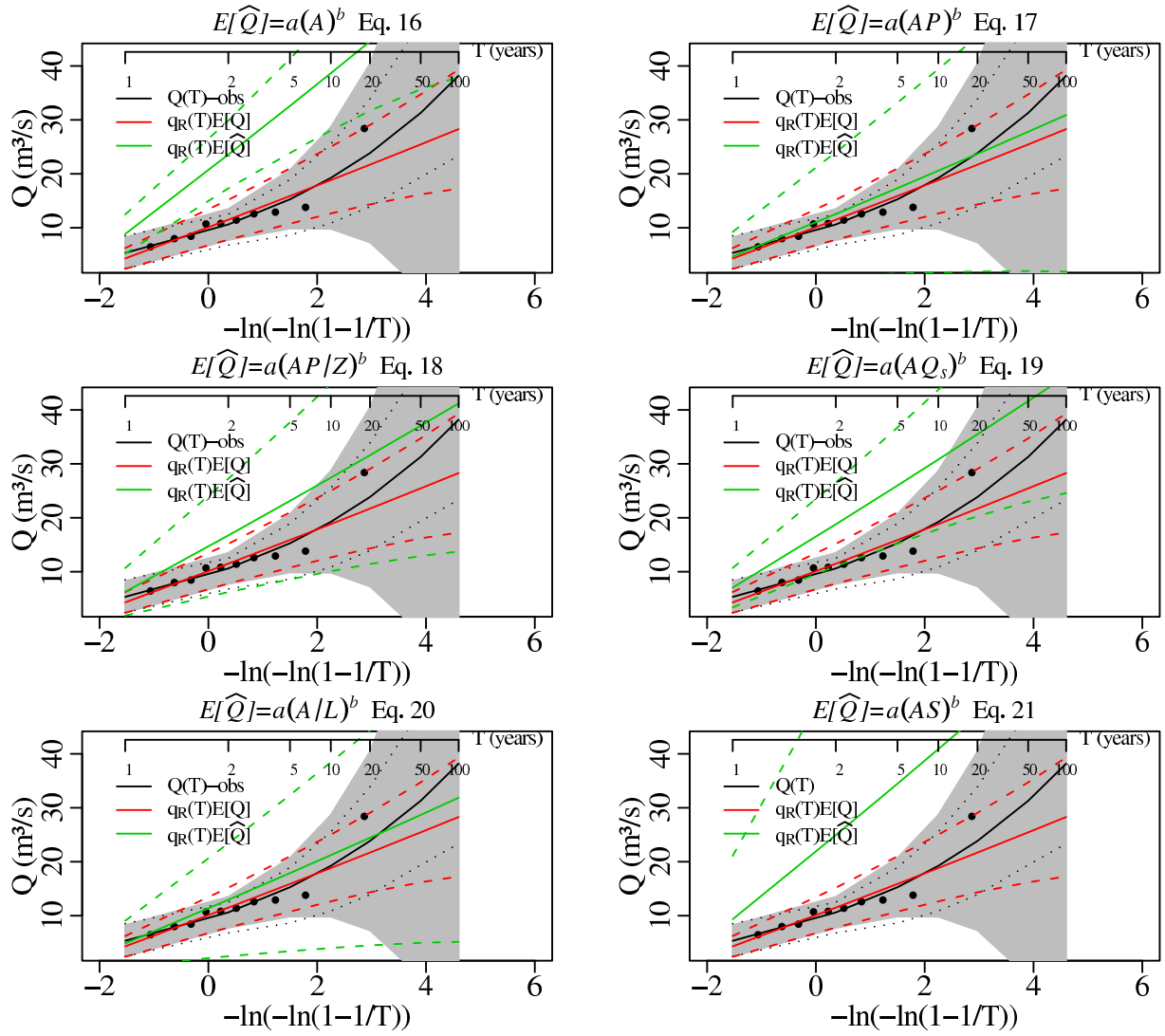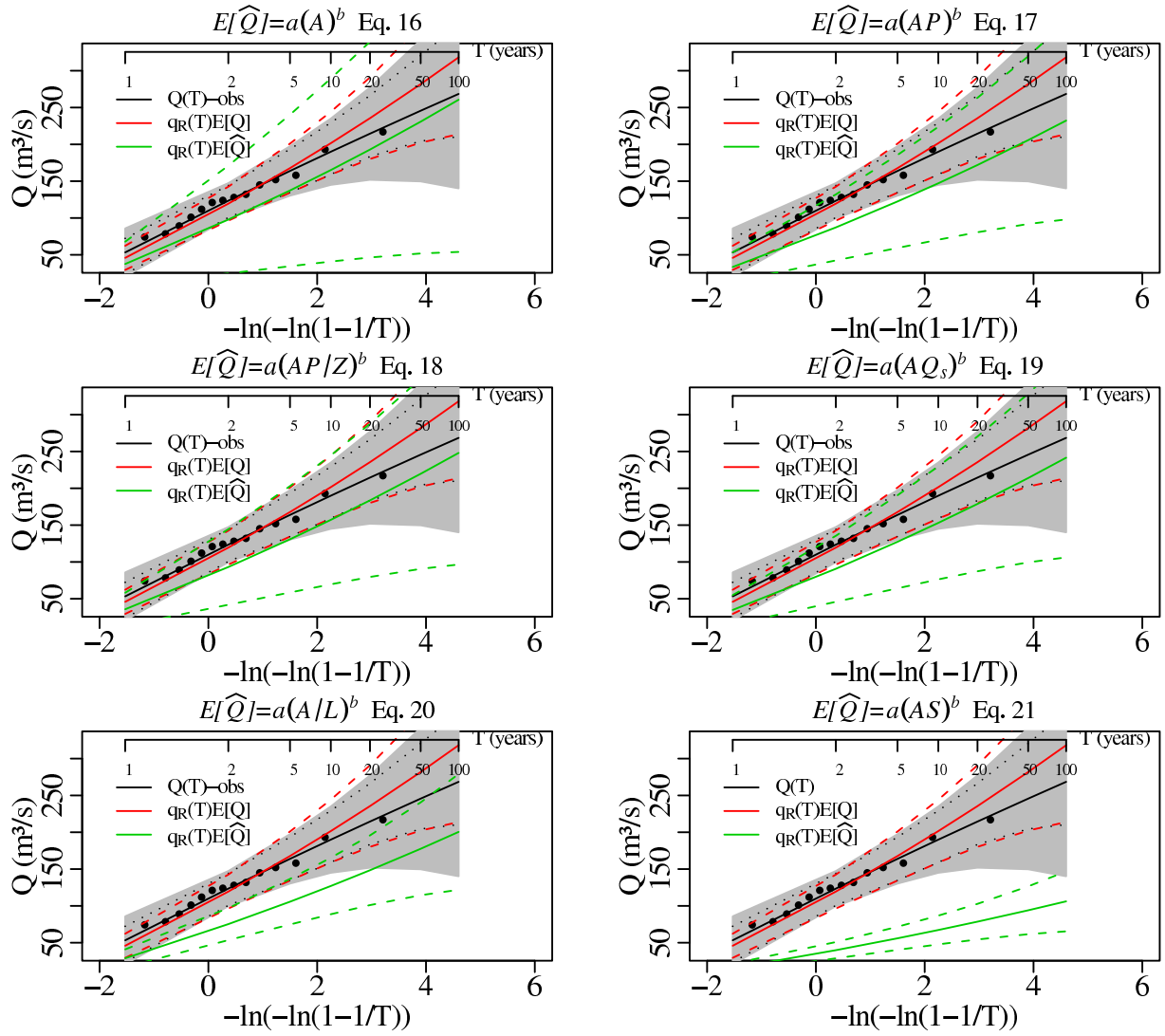
Distribution of annual max. instantaneous Q, VHM 92
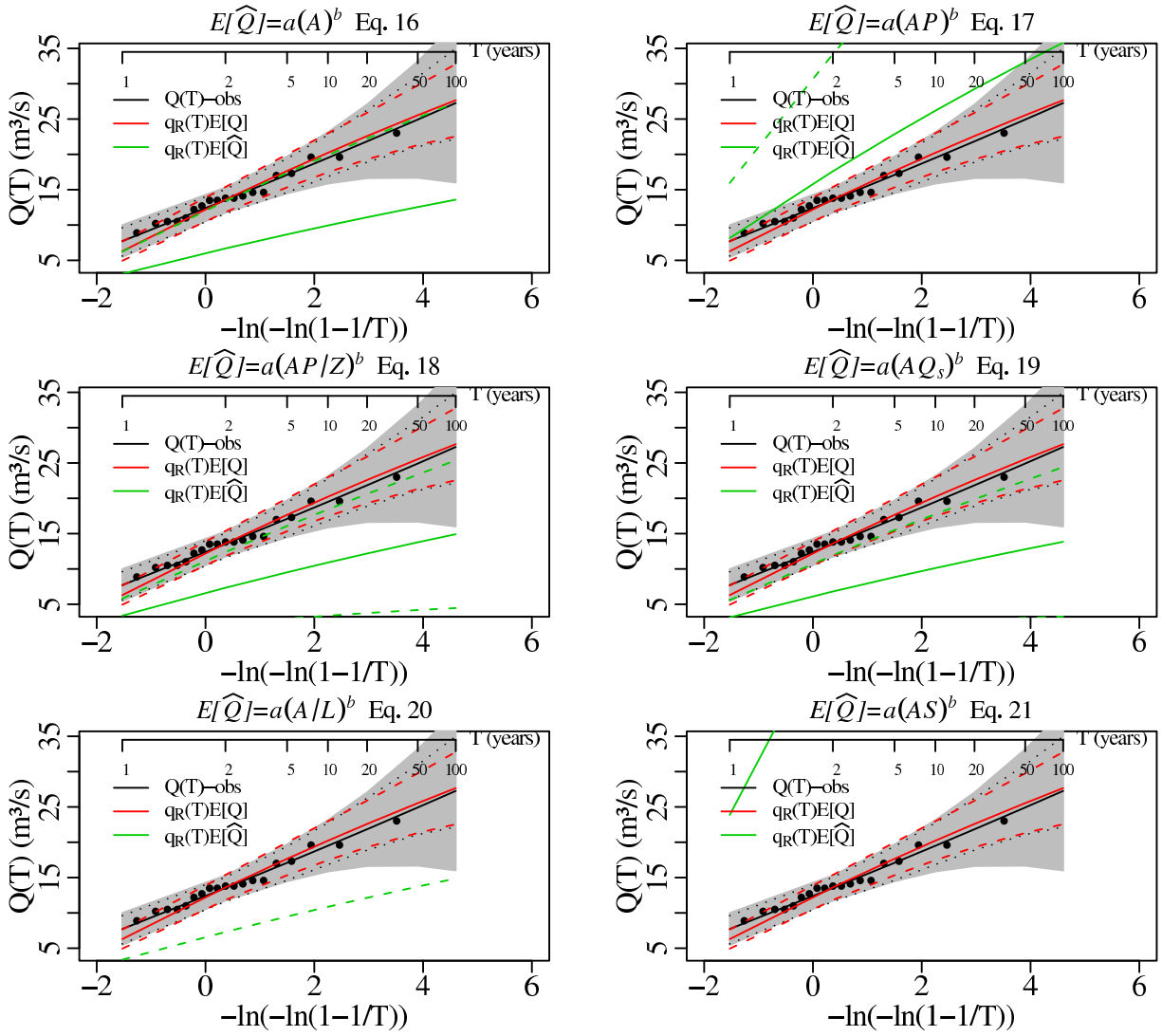
Figure I.3. Observed and estimated flood CDFs for annual maximum instantaneous flood at VHM-92. See caption of Fig. I.1.
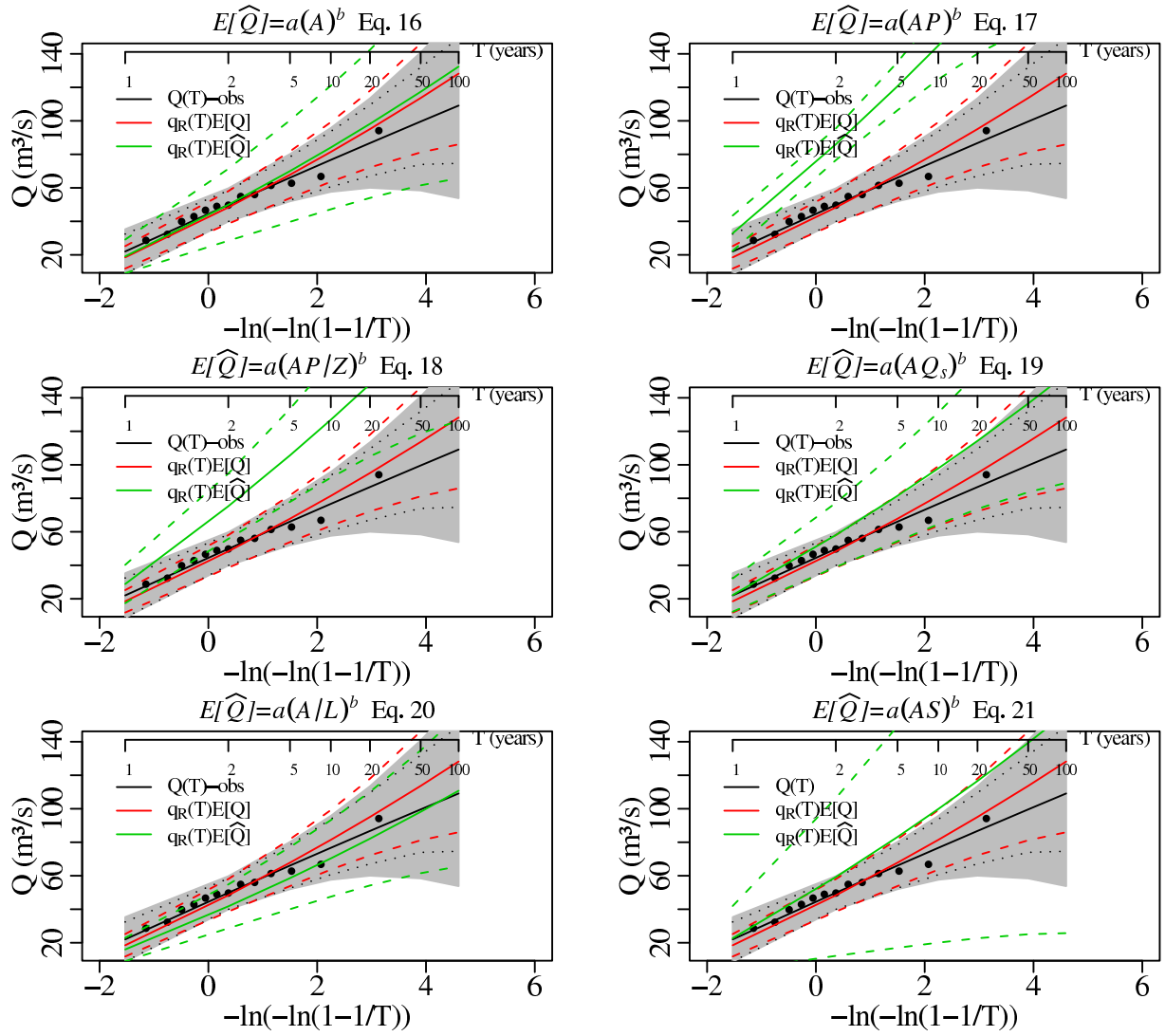
Distribution of annual max. instantaneous Q, VHM 200
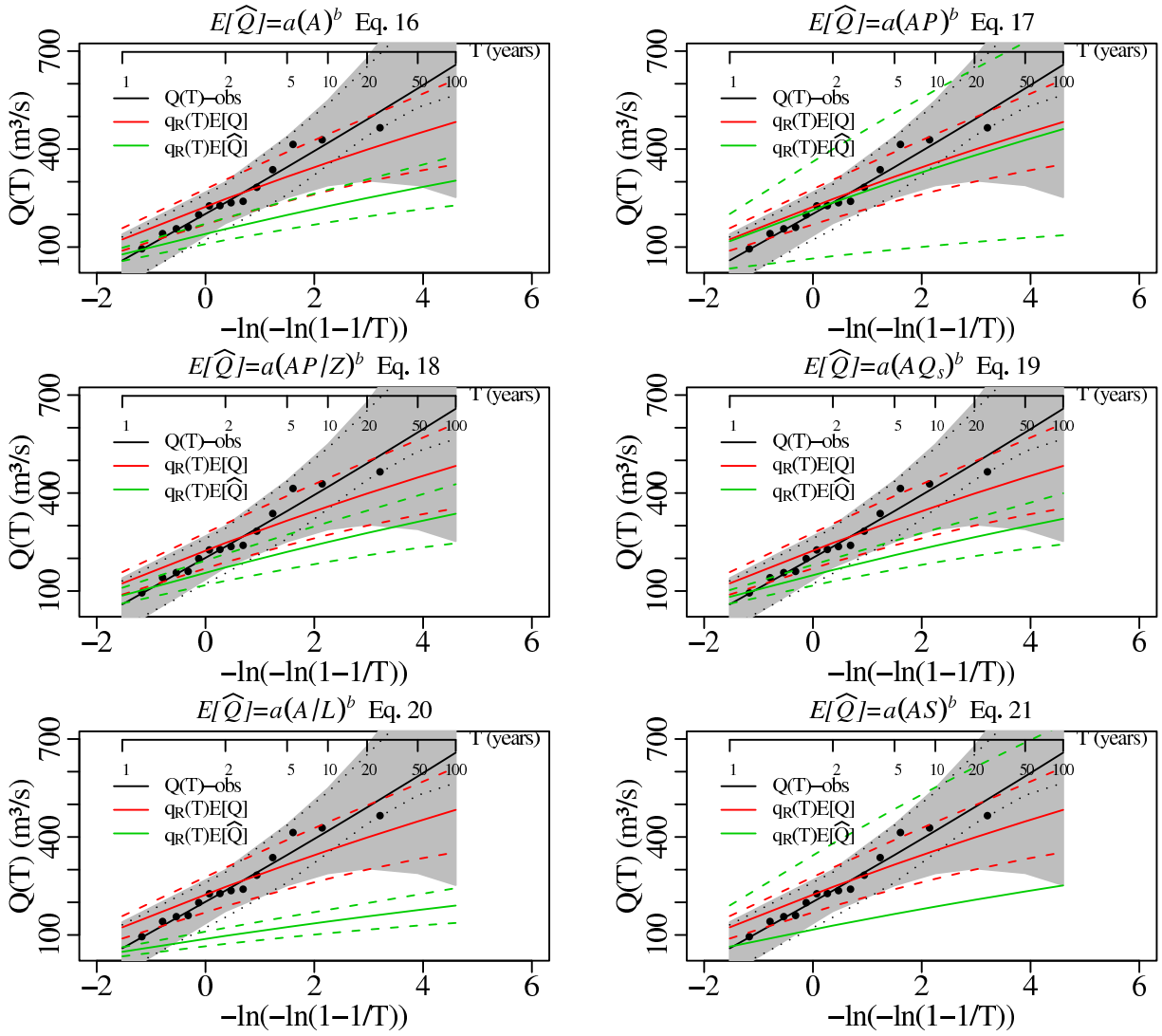
Figure I.4. Observed and estimated flood CDFs for annual maximum instantaneous flood at VHM-200. See caption of Fig. I.1.
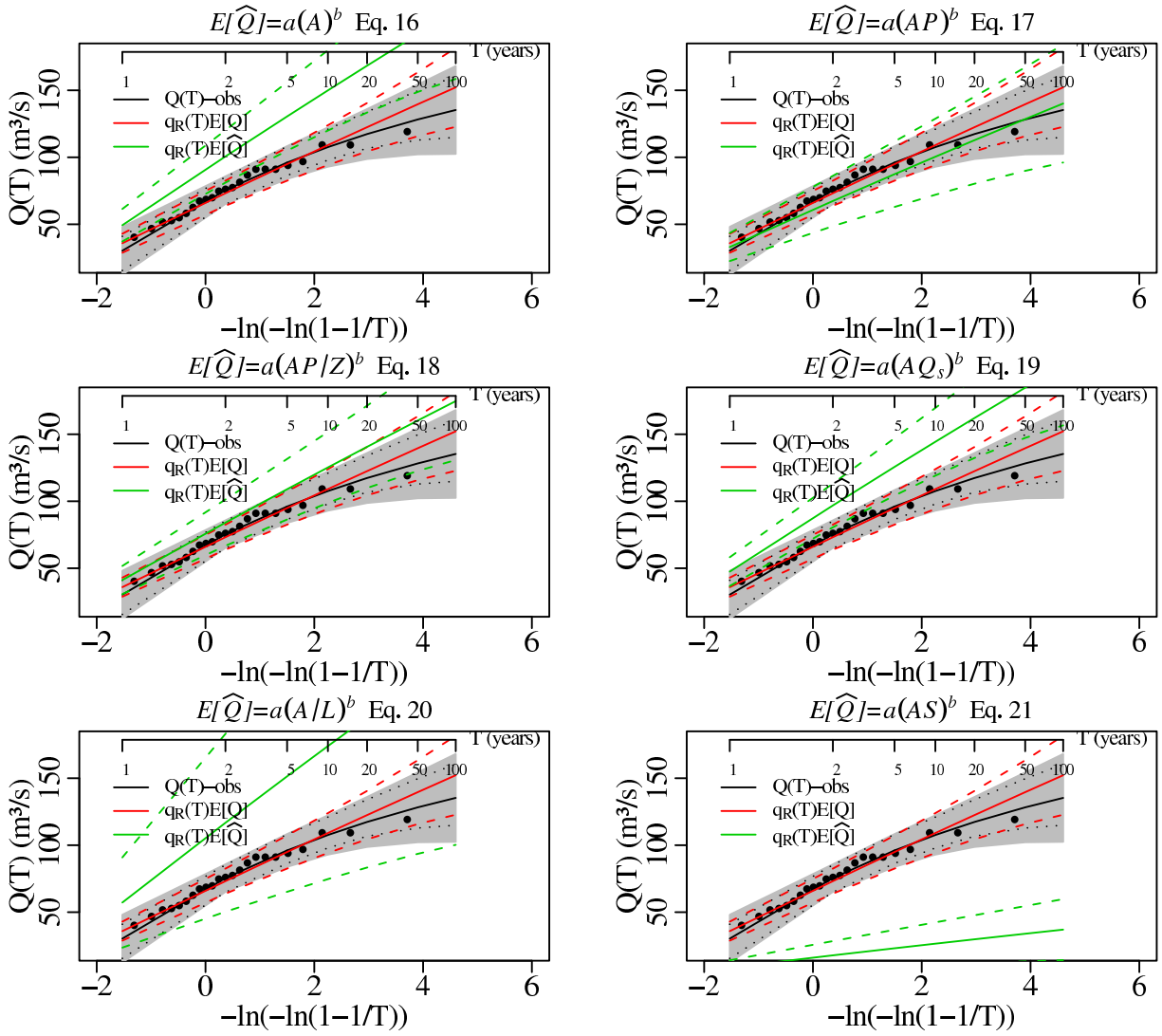
Figure I.5. Observed and estimated flood CDFs for annual maximum instantaneous flood at VHM-45. See caption of Fig. I.1.

Distribution of annual max. instantaneous Q, VHM 12
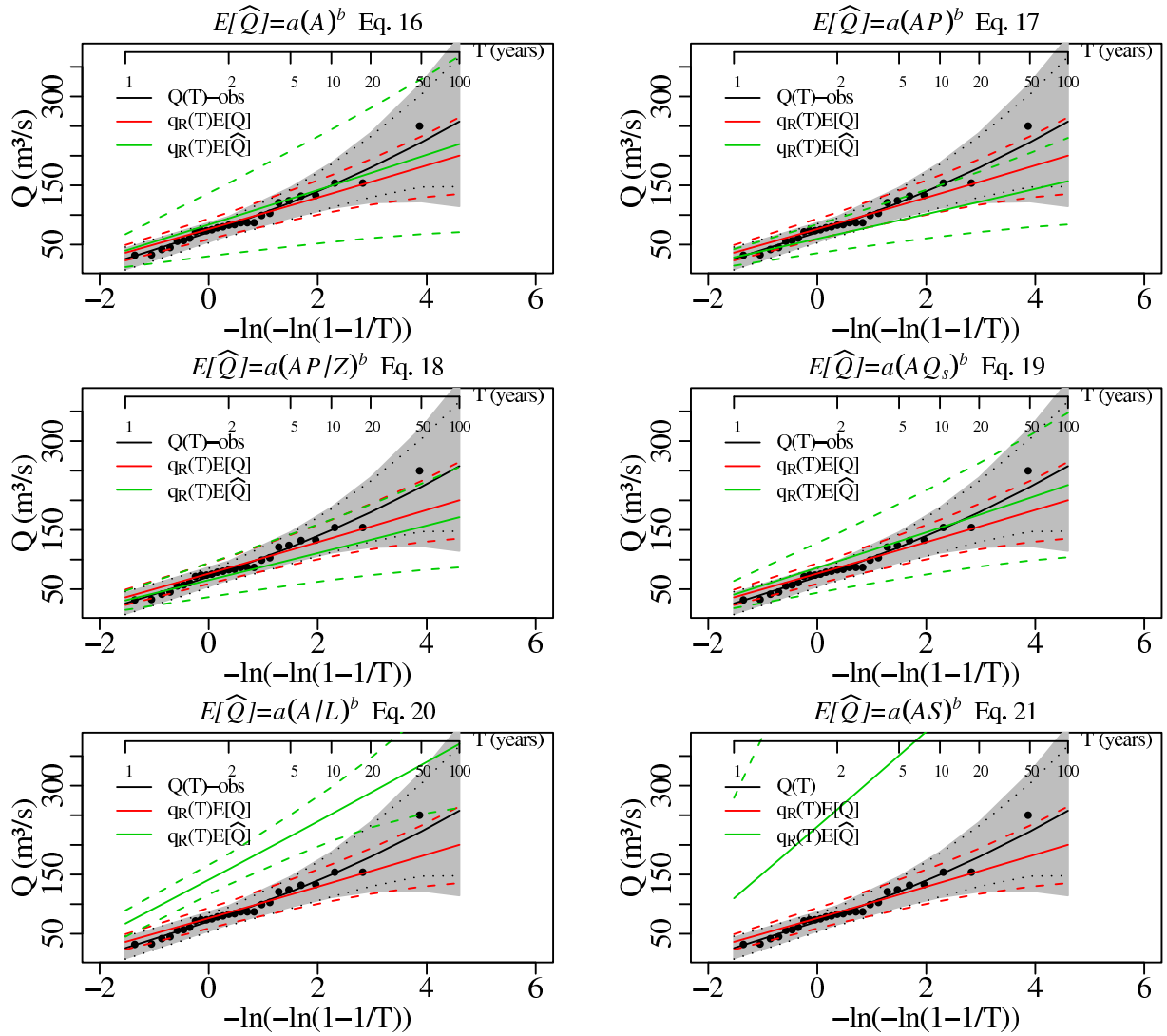
Figure I.6. *Observed and estimated flood CDFs for annual maximum instantaneous flood at VHM-12. See caption of Fig. I.1.*

Distribution of annual max. instantaneous Q, VHM 19
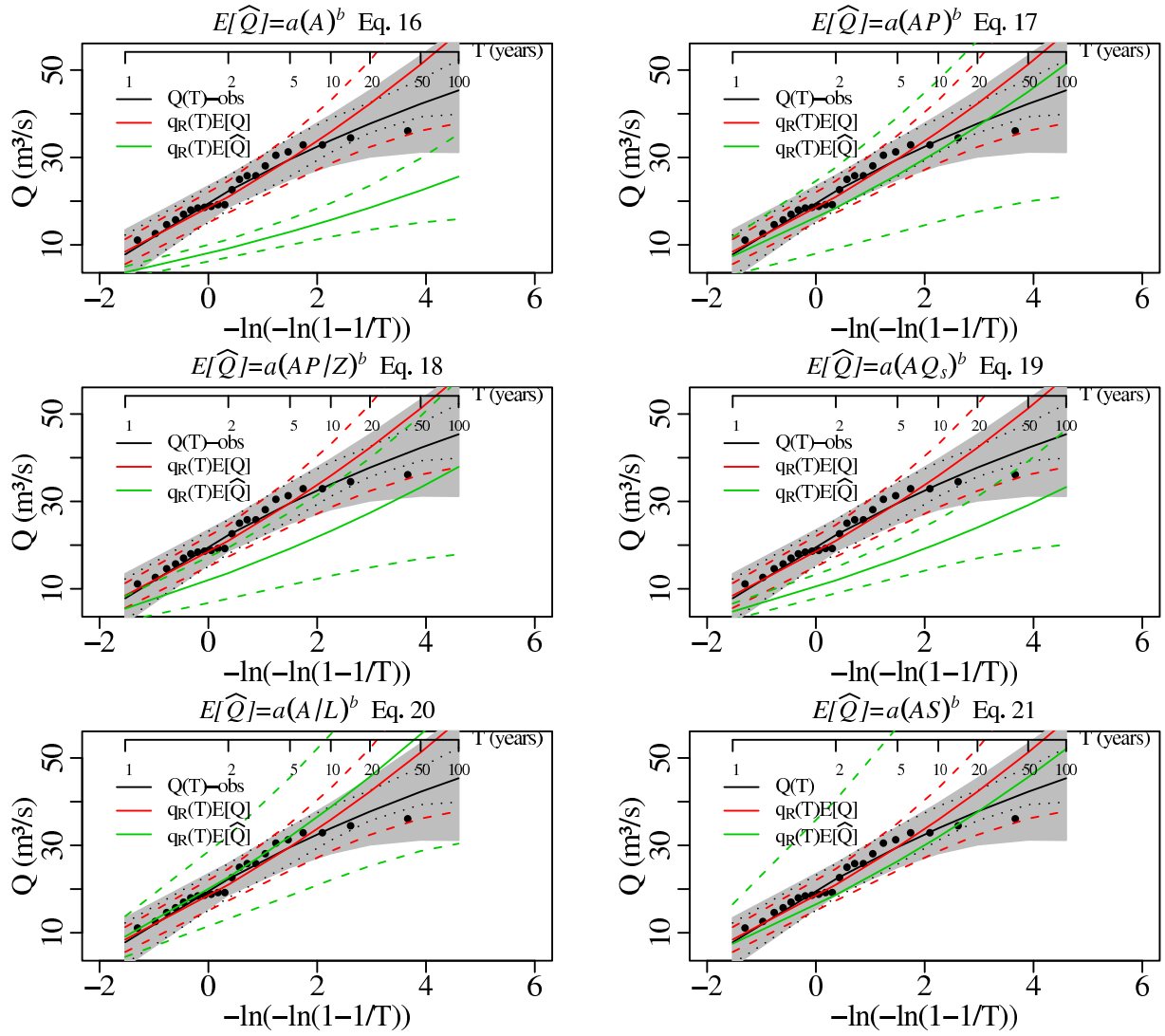
Figure I.7. Observed and estimated flood CDFs for annual maximum instantaneous flood at VHM-19. See caption of Fig. I.1.

Distribution of annual max. instantaneous Q, VHM 38

Figure I.8. Observed and estimated flood CDFs for annual maximum instantaneous flood at VHM-38. See caption of Fig. I.1.
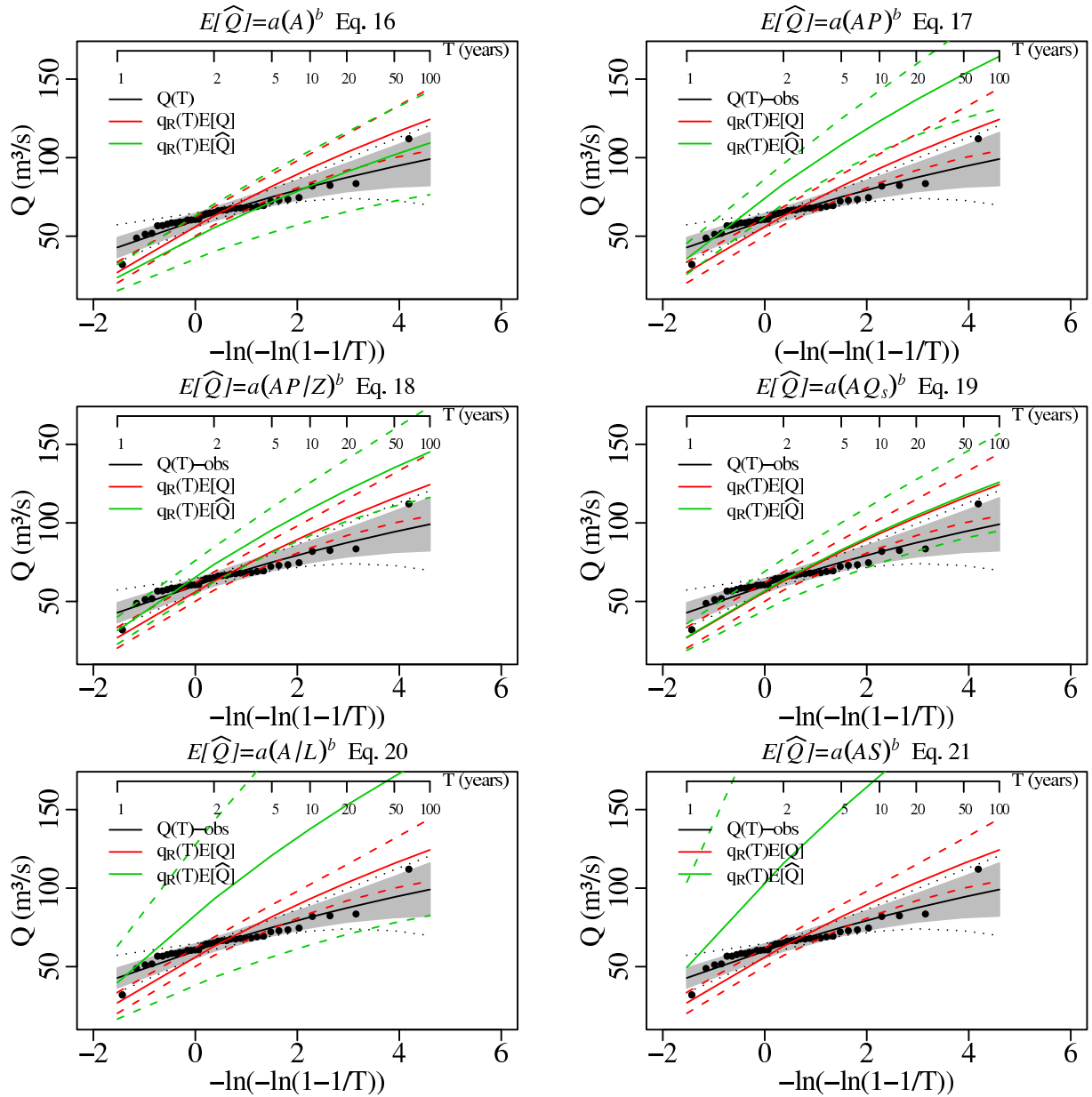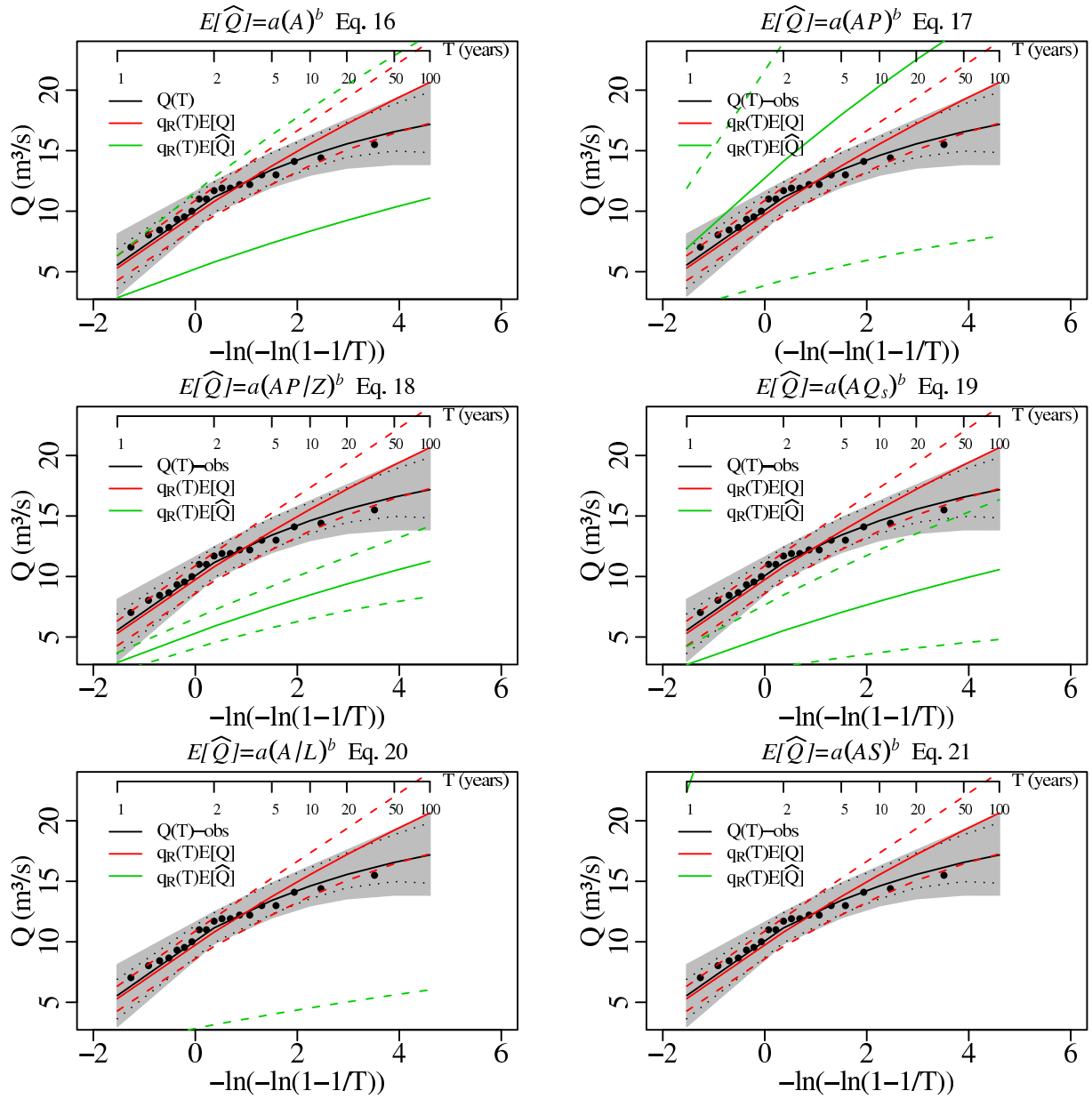
Figure I.9. Observed and estimated flood CDFs for annual maximum instantaneous flood at VHM-198. See caption of Fig. I.1.

Distribution of annual max. instantaneous Q, VHM 204

Figure I.10. Observed and estimated flood CDFs for annual maximum instantaneous flood at VHM-204. See caption of Fig. I.1.

Appendix II. Observed and estimated flood cumulative distribution functions (CDFs) for annual maximum daily flood using a regional growth curve and 6 different index flood models
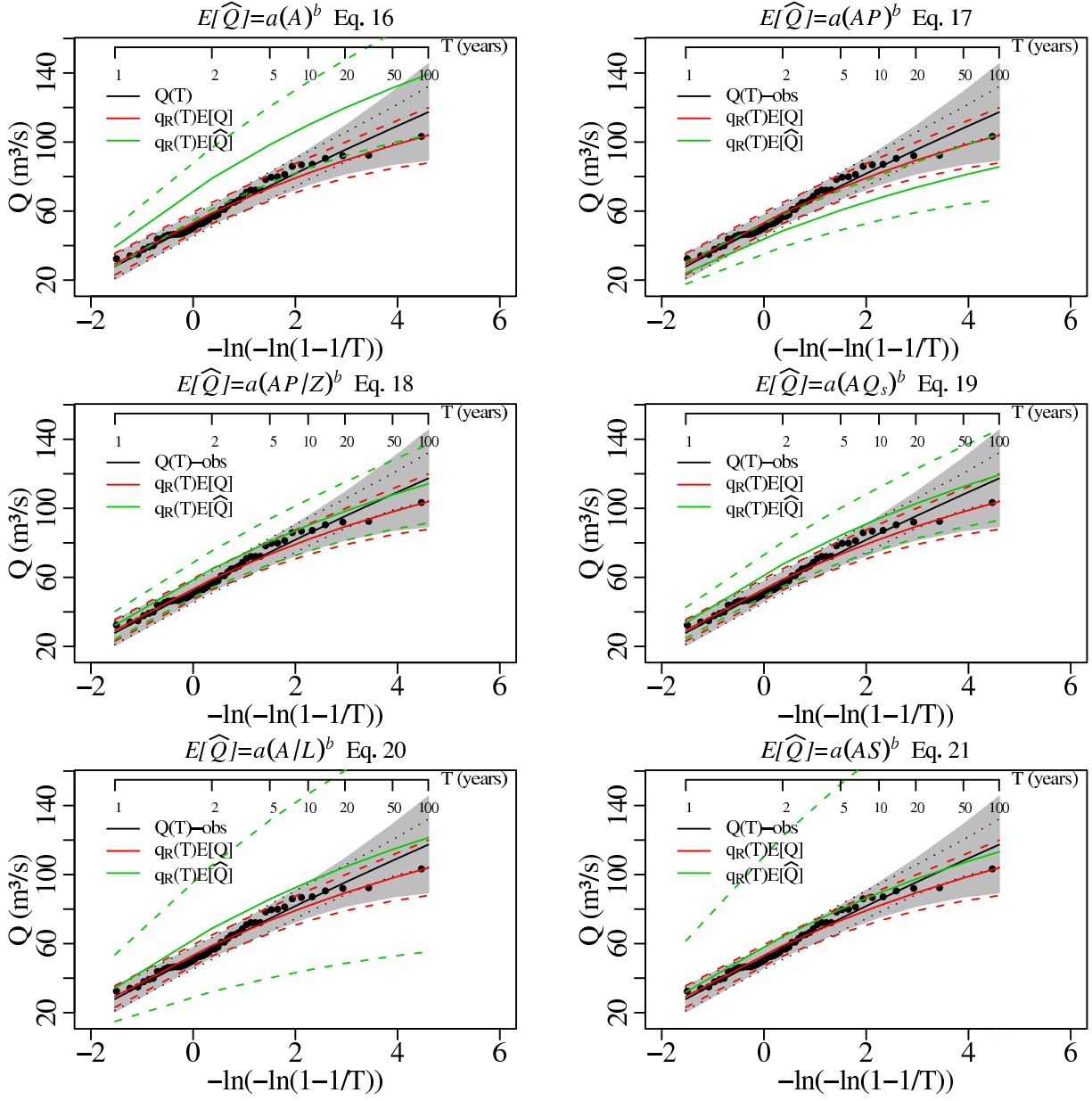
Figure II.1. Observed and estimated flood CDFs for annual maximum daily flood at VHM-10. The solid black line represents the reference GEV/PWM distribution estimated with the observed flood sample, the grey shaded region represents the 95% confidence interval and the dotted black line the 95% bootstrap confidence interval. The solid red line corresponds to the GEV distribution estimated with Eq. (1), by the product of the regional growth curve $q_R(T)$ and an index flood estimated by the observed sample mean $E[\widehat{\widehat{Q}}_i]$ (Eq. 4). The solid green line corresponds to the GEV distribution estimated with Eq. (1), by the product of the regional growth curve $q_R(T)$ and an index flood estimated by the linear model $\widehat{E[Q_i]} = a_0 x_1^{a_1} x_2^{a_2} x_3^{a_3} \ldots x_l^{a_l}$ (Eqs. 16–21). The colored dashed lines give their respective 95% confidence intervals.

Distribution of annual max. daily Q, VHM 51

Figure II.2. Observed and estimated flood CDFs for annual maximum daily flood at VHM-51. See caption of Fig. II.1.

51

Figure II.3. Observed and estimated flood CDFs for annual maximum daily flood at VHM-92. See caption of Fig. II.1.

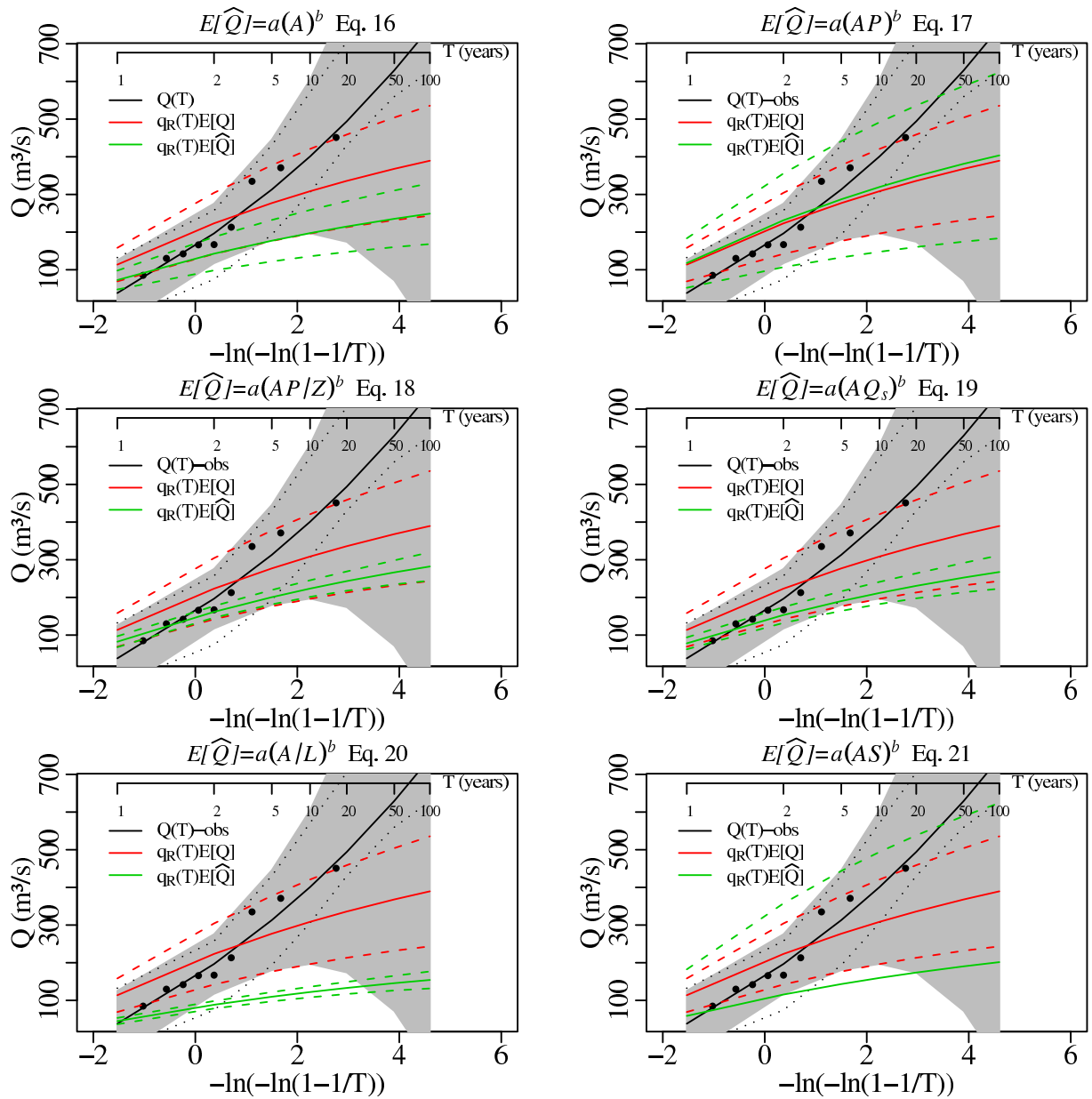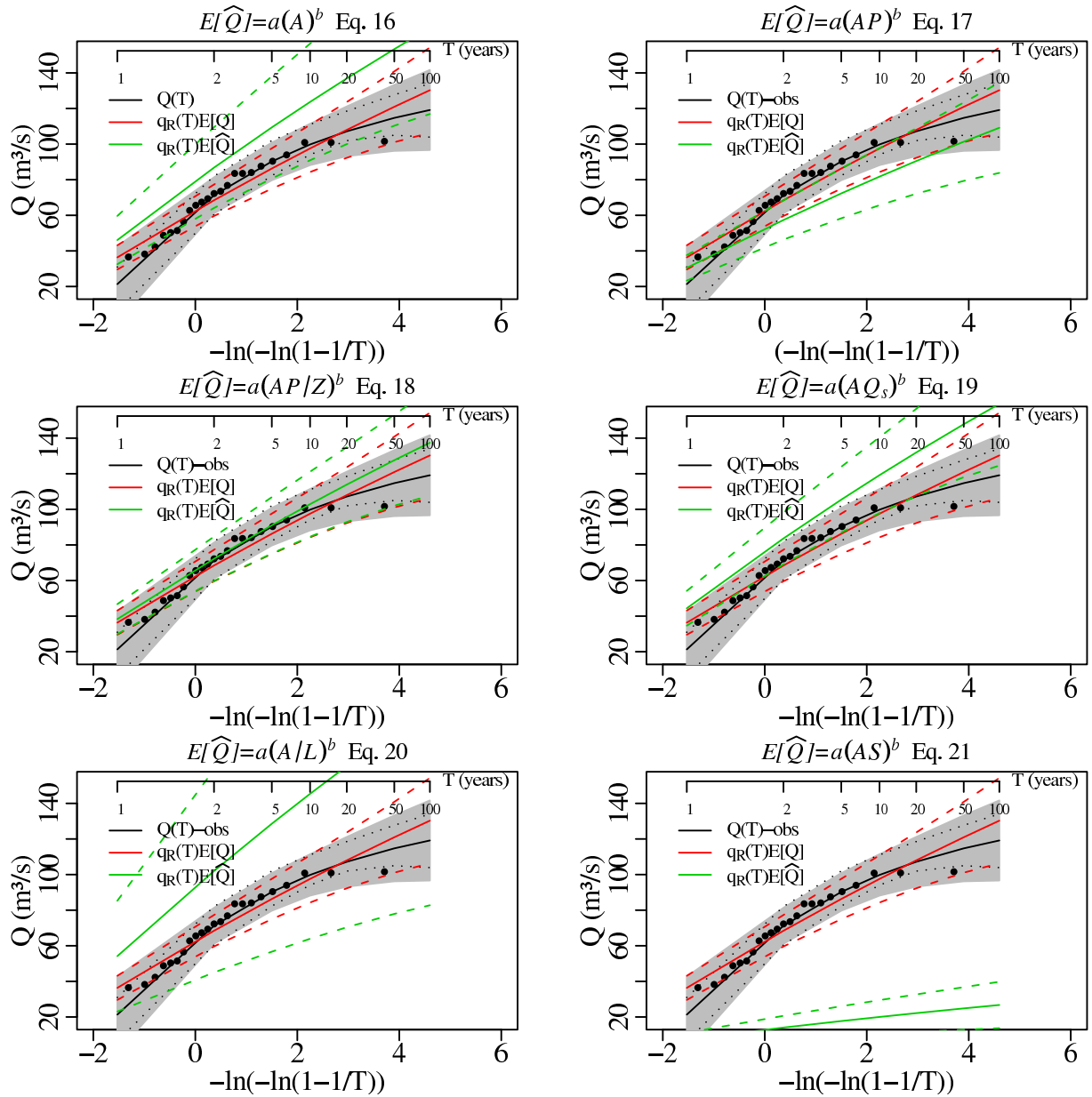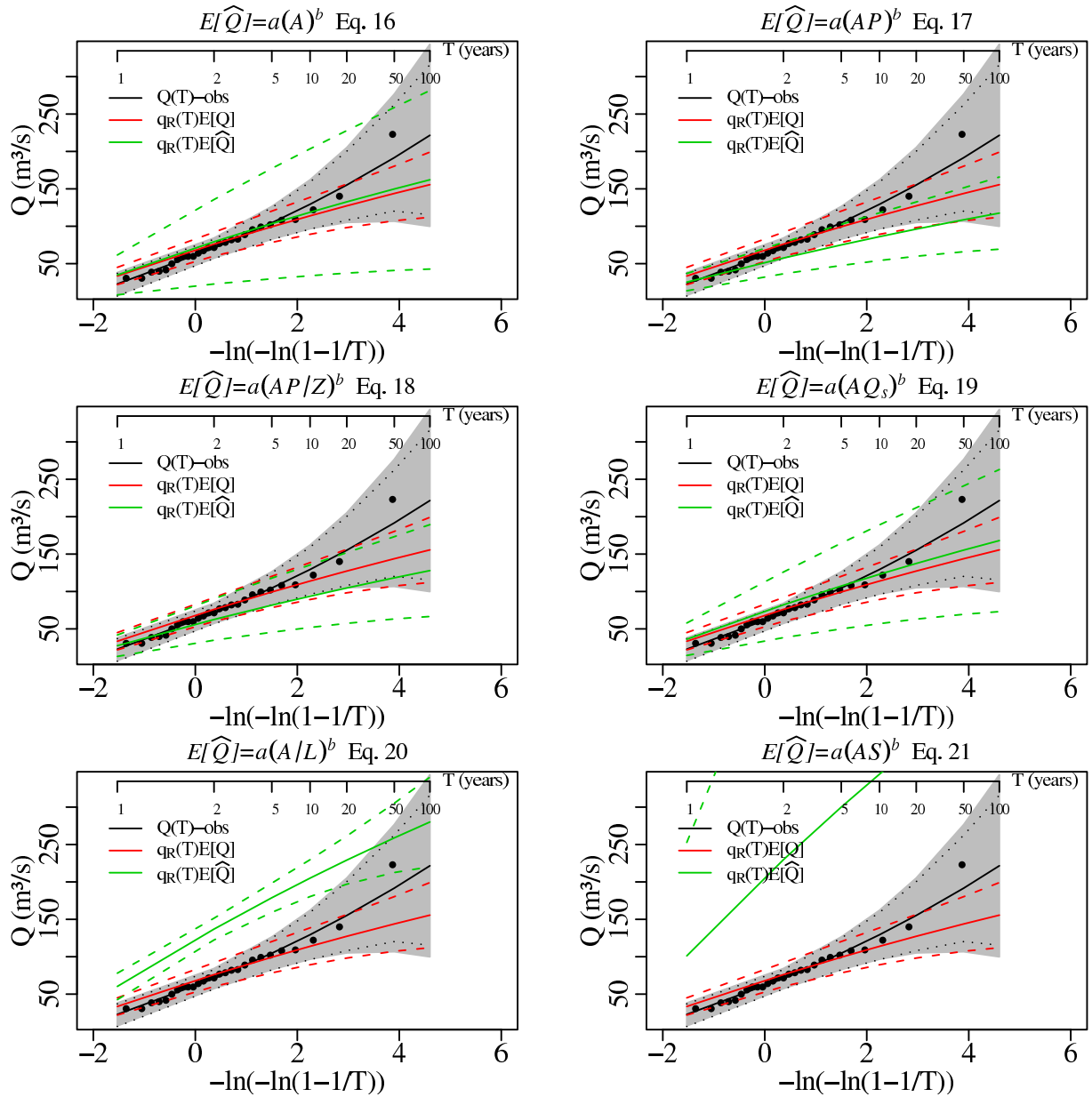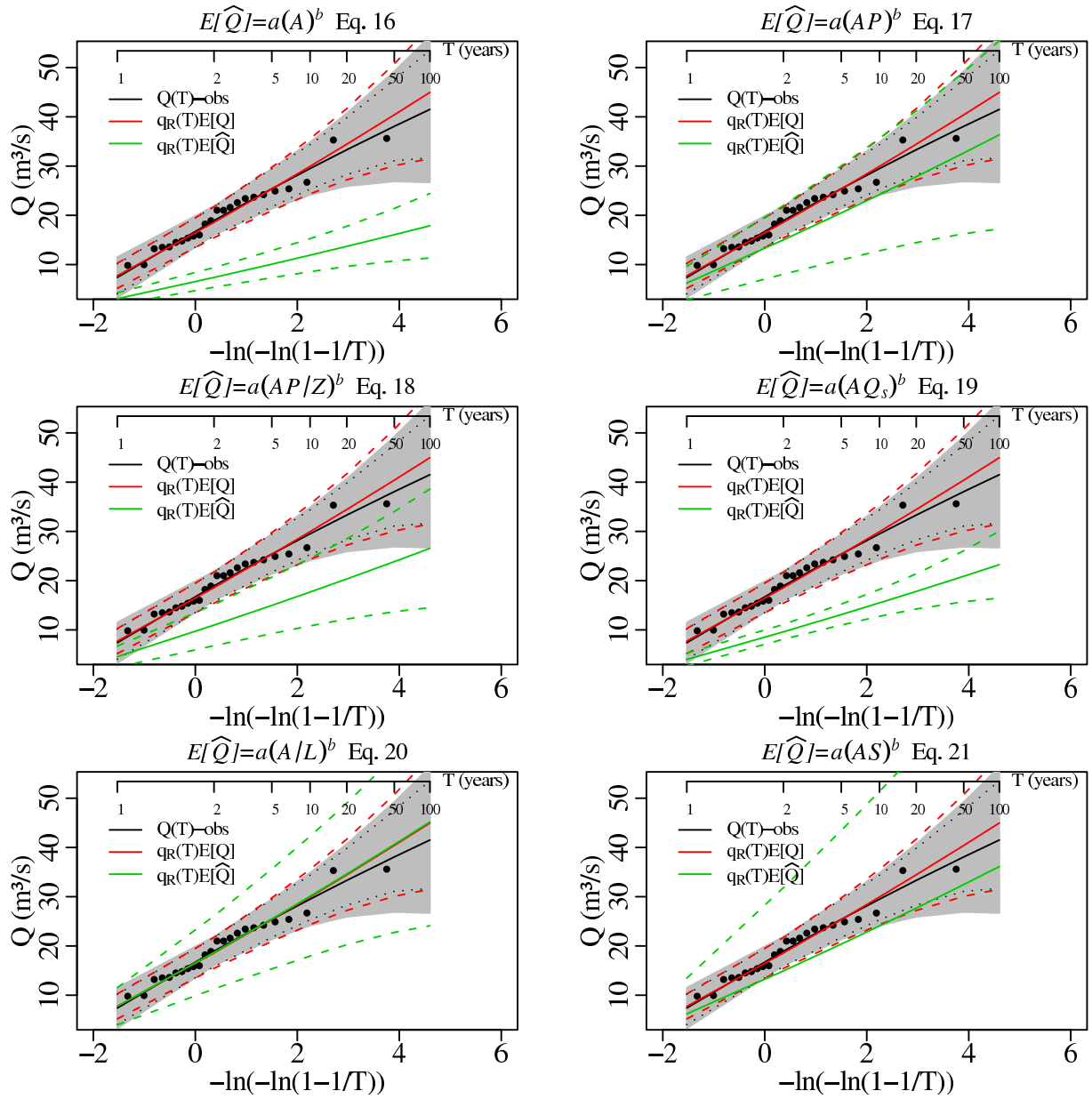**Distribution of annual max. daily Q, VHM 200**

Figure II.4. Observed and estimated flood CDFs for annual maximum daily flood at VHM-200. See caption of Fig. II.1.
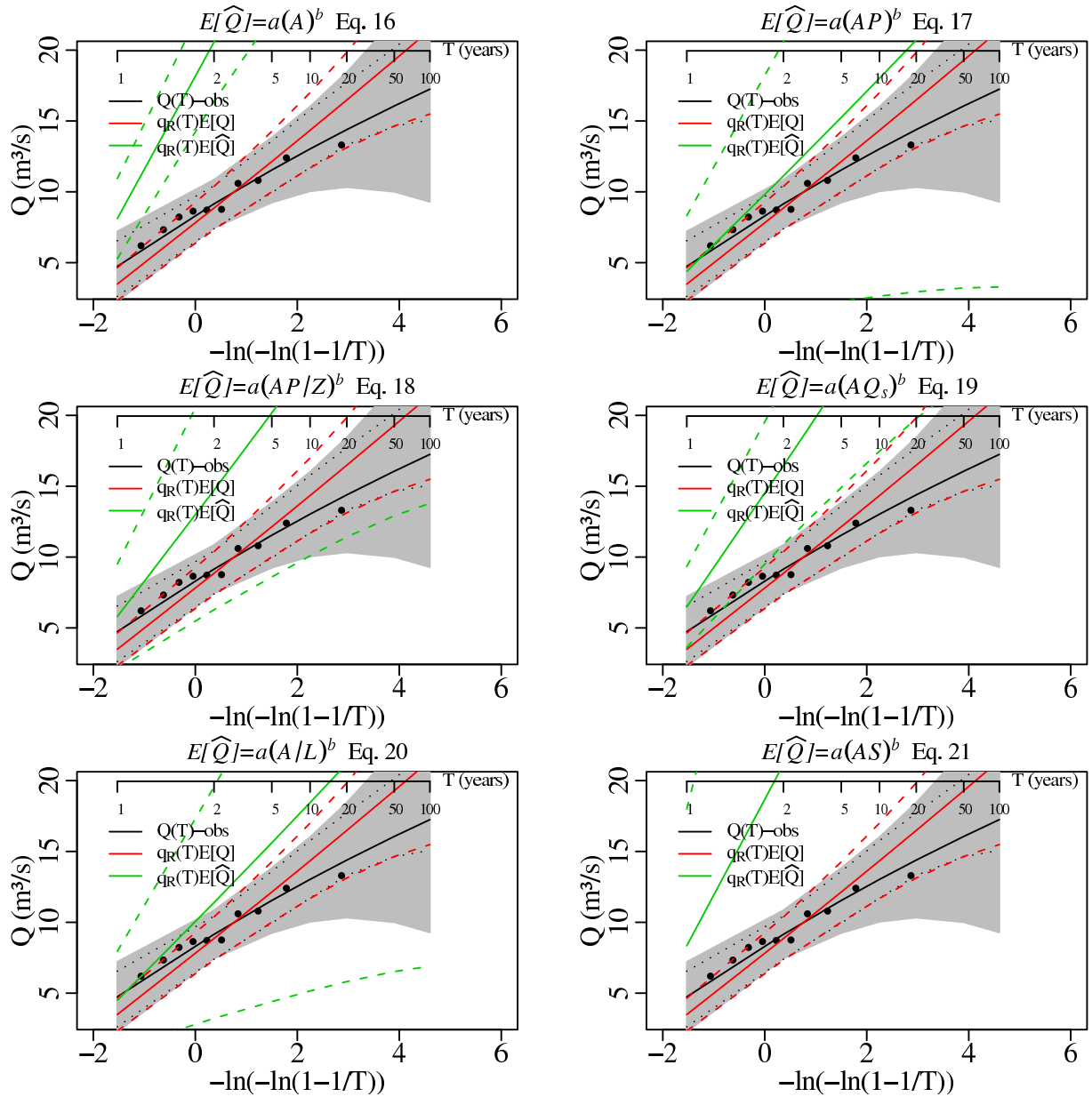
Figure II.5. Observed and estimated flood CDFs for annual maximum daily flood at VHM-45. See caption of Fig. II.1.
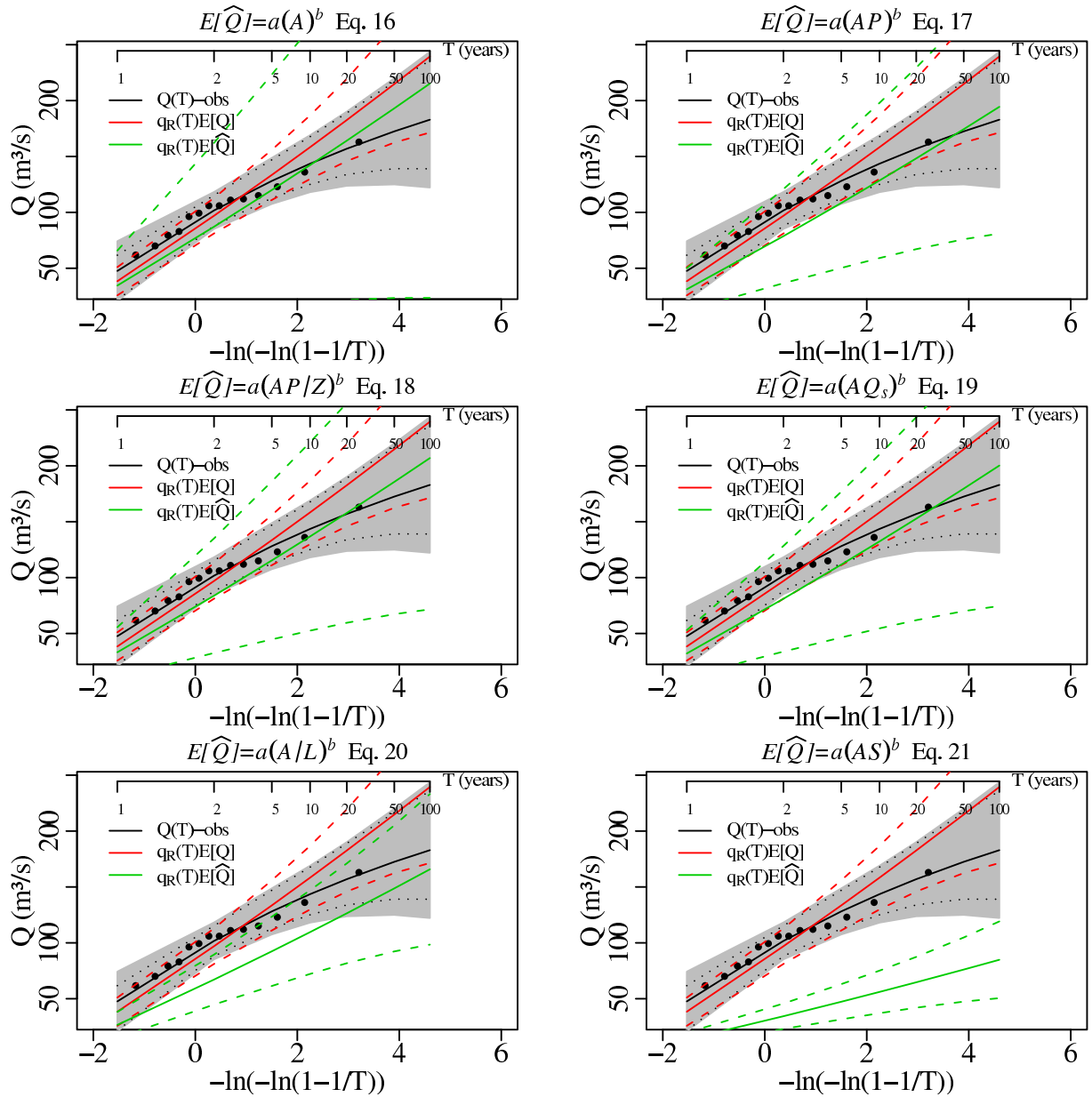
Distribution of annual max. daily Q, VHM 12

Figure II.6. Observed and estimated flood CDFs for annual maximum daily flood at VHM-12. See caption of Fig. II.1.

Figure II.7. Observed and estimated flood CDFs for annual maximum daily flood at VHM-19. See caption of Fig. II.1.

Figure II.8. Observed and estimated flood CDFs for annual maximum daily flood at VHM-38. See caption of Fig. II.1.

Figure II.9. Observed and estimated flood CDFs for annual maximum daily flood at VHM-198. See caption of Fig. II.1.
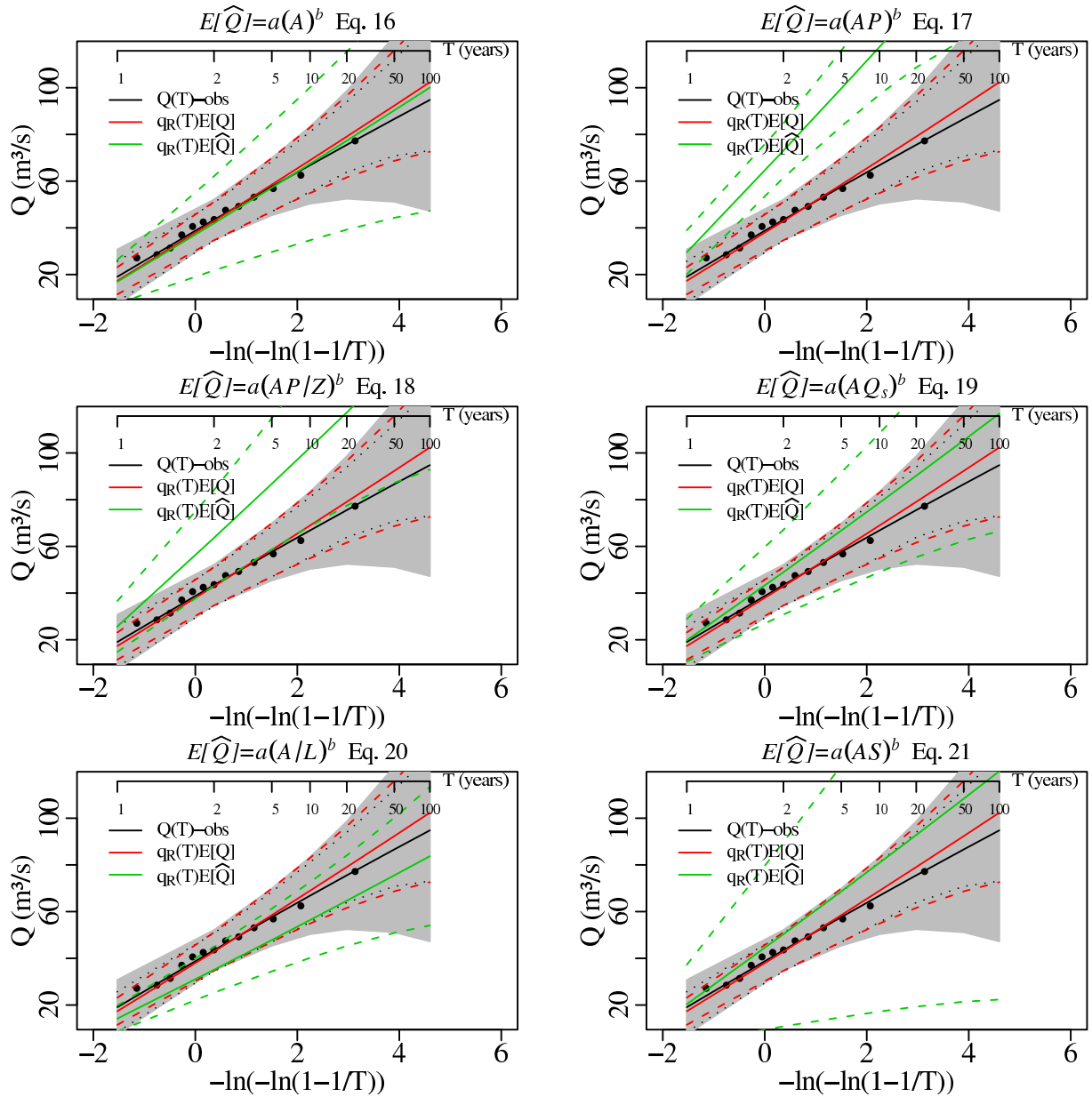
Figure II.10. Observed and estimated flood CDFs for annual maximum daily flood at VHM-204. See caption of Fig. II.1.